NPS ARCHIVE
1962
REED, R.

DUDLEY KNOX LIBRARY
NAVAL POSTGRADUATE SCHOOL
MONTEREY CA 93943-5101

Library
U. S. Naval Postgraduate School
Monterey, California

EFFECT OF A CADMIUM CONTROL ROD ON THE NEUTRON DENSITY IN A SUBCRITICAL REACTOR

EFFECT OF A CADMIUM CONTROL ROD ON THE NEUTRON DENSITY IN A SUBCRITICAL REACTOR

By

RICHARD W. REED, B.S.

THESIS

Presented to the Faculty of the Graduate School of
The University of Texas in Partial Fulfillment
of the Requirements

For the Degree of

MASTER OF ARTS

THE UNIVERSITY OF TEXAS

August 1962

PS Archive
162
eed, R

Thesis
~~R2698~~

DUDLEY KNOX LIBRARY
NAVAL POSTGRADUATE SCHOOL
MONTEREY CA 93943-5101

Library
U. S. Naval Postgraduate School
Monterey, California

PREFACE

If experimental work is to be accomplished involving the use of a nuclear reactor, accurate knowledge concerning the density of neutrons at various locations within the reactor is a necessity, whether the reactor be critical or subcritical.

The neutron density distribution in a given reactor can be estimated mathematically by the use of several techniques including transport theory, multigroup diffusion theory, and single group diffusion theory. Of these various mathematical theories, the single group diffusion is the only one amenable to hand calculations. Unfortunately, however, diffusion theory is also the least accurate of the three named, although it does provide a good first approximation to the actual neutron density distribution within a reactor.

In order to accurately determine the neutron density distribution within a reactor, experimental measurements must be conducted using one of the various methods available for such measurements. One of the most convenient methods is that of foil activation measurements.

Control rods made of materials which can absorb great numbers of neutrons are used to control the neutron distribution within reactors. In critical systems, such control rods are, of course, necessary for safe and proper operation of the reactor.

The University of Texas maintains a subcritical reactor which is used for teaching purposes and for research. The purpose of this thesis is to accurately determine the effect of a pure cadmium control rod on the neutron density distribution in this reactor.

The neutron density distribution is determined by foil activation measurements both with and without the cadmium control rod. Single group diffusion theory is used to predict the distribution mathematically, and the theoretical distributions are compared with the experimentally determined ones.

The experimentally determined neutron density distribution without the control rod is compared with the distribution with the cadmium control rod in place in order to clearly show the effect of the rod on the neutron density.

The author wishes to express his appreciation to Dr. R. N. Little for his advice and guidance during his supervision of this research and to Dr. J. A. Scanlan for

his many helpful suggestions concerning the writing of the thesis. Sincere gratitude is also due Mr. S. C. Mathur and Mr. C. J. Spahn for their patient, expert, and time consumming assistance with the equipment used in this experiment.

Since the writing of this thesis marks the end of a long, hard, three year struggle, the author feels that it should at least have a dedication. Therefore this writing is dedicated to the person who has provided the encouragement and the understanding which is so necessary in this type of work-----to my wife, Patti.

R. W. R.

The University of Texas
Austin, Texas
August, 1962

TABLE OF CONTENTS

Chapter Page

I. THEORY 1

A. One Velocity Group Diffusion Theory Approximation Without Control Rods 1

B. One Velocity Group Diffusion Theory Approximation with Control Rod 13

II. NEUTRON FLUX MEASUREMENT BY THE ACTIVATION METHOD 19

A. General 19

B. Use of Dysprosium Foils for Thermal Neutron Detection 20

C. Determination of Absolute Thermal Neutron Flux from Measured Activity 28

III. EXPERIMENTAL APPARATUS AND PROCEDURE 37

A. Reactor, External Neutron Source, and Control Rods 37

B. Foils 44

C. Beta Counting Equipment 48

D. Experimental Procedure 54

IV. DATA AND GRAPHS 57

V. RESULTS 65

APPENDIX A 68

APPENDIX B 78

BIBLIOGRAPHY 84

CHAPTER I

THEORY

A. One Velocity Group Diffusion Theory Approximation without Control Rods[1]

In the single velocity group diffusion theory it is assumed that all neutrons in the system being studied have the same velocity, which in the present case is 2200 meters per second, the velocity of thermal neutrons. If the neutron population is described in terms of the neutron density, $n(r,t)$, where

$n(r,t) \equiv$ number of neutrons of speed v per unit volume around space point r at time t,

then the neutron flux, $\phi(r,t)$, is expressed in terms of $n(r,t)$ by the usual definition

$$\phi(r,t) \equiv vn(r,t)$$

where, in this case, all values are for thermal neutrons and v is constant and uniform throughout the reactor.

A verbal statement of the neutron balance equation for a differential volume element, dV, includes a term to

---

[1] R. V. Meghreblian and D. K. Holmes, Reactor Analysis (New York: McGraw-Hill Book Co., 1960), Chap. 5.

account for the net gain or loss through the boundaries of the volume element, and is

$$\begin{bmatrix}\text{Rate of increase}\\ \text{of the neutron}\\ \text{density in dV}\\ \text{about r}\end{bmatrix} =$$

$$\begin{bmatrix}\text{number of}\\ \text{neutrons pro-}\\ \text{duced in dV}\\ \text{per unit time}\end{bmatrix} - \begin{bmatrix}\text{number of}\\ \text{neutrons ab-}\\ \text{sorbed in dV}\\ \text{per unit time}\end{bmatrix} - \begin{bmatrix}\text{net number of}\\ \text{neutrons escap-}\\ \text{ing from dV}\\ \text{per unit time}\end{bmatrix}$$

This statement, in mathematical form, becomes the equation

$$\frac{\partial n}{\partial t}dV = S(r,t)dV - \Sigma_a \phi(r,t)dV - \mathcal{L}(r,t)dV$$

where $S(r,t)$ is called the source function and denotes the number of neutrons produced per unit time in dV, and the term $\mathcal{L}(r,t)$ is called the leakage function and denotes the let loss of neutrons from dV due to diffusion through the boundaries.

In diffusion theory the leakage term becomes

$$\mathcal{L}(r,t) = - D\nabla^2\phi\ (r,t)$$

and the neutron balance equation becomes, under steady state conditions for which $n(r,t)$ is constant,

$$- D\nabla^2 \phi(r) + \Sigma_a \phi(r) = S(r).$$

In this equation D is called the diffusion coefficient and is defined to be

$$D \equiv \frac{\lambda_{tr}}{3} = \frac{1}{3[\Sigma_{total} - \Sigma_s (\cos\theta)_{avg}]}$$

where λ_{tr} is the transport mean free path for the medium containing the volume element dV for which the equation was derived. Σ_a is the macroscopic absorption cross section for this medium, and S(r) is the source term. As indicated above

$$\lambda_{tr} = \frac{1}{[\Sigma_{total} - \Sigma_s (\cos\theta)_{avg}]}$$

where Σ_s is the macroscopic scattering cross section for the medium, $(\cos\theta)_{avg} = 2/3A$ and is the average scattering angle for neutrons involved in scattering collisions with nuclei of the medium. Σ_{total} is the sum of Σ_s and Σ_a.

The net neutron current through a given area located at r is given by the vector equation

$$\vec{J}(r) = -D\nabla\phi(r).$$

The partial neutron currents through an area are defined by the equations

$$j_+(r) = \frac{1}{4}\,\phi(r) - \frac{D}{2}\,|\nabla\phi(r)|\cos\,\theta_n$$

and

$$j_-(r) = \frac{1}{4}\,\phi(r) + \frac{D}{2}\,|\nabla\phi(r)|\cos\,\theta_n$$

where θ_n is the angle between the unit vector normal to the area and the unit vector parallel to the vector $\nabla\phi(r)$. The difference of the partial currents is equal to $\vec{J}(r)$. In other words,

$$\vec{J}(r) \equiv j_+(r) - j_-(r).$$

The boundary conditions which must be used in obtaining a solution for the above diffusion theory neutron balance equation are as follows:

(1) $\phi(r)$ must be finite and nonnegative in all regions of the medium in which the diffusion equation applies.

(2) At any interface between two media with different diffusion coefficients, the partial currents must be continuous through the interface. If there is

no external source at an interface, then the neutron flux, $\phi(r)$, and the net current, $J(r)$, must be continuous at the interface.

(3) The flux $\phi(r)$ must vanish at some finite distance outside the boundary or else the partial current from the area outside the boundary must be zero. In diffusion theory, the distance beyond the reactor boundary at which $\phi(r) = 0$ is called the extrapolation distance, d ($= 0.7104\ \lambda_{tr}$).

Two assumptions were made in this treatment concerning the reactor assembly without the control rod. It was assumed that the air gap along the central axis of the core did not exist. This air gap actually represented only approximately 1.20 per cent of the volume of the core; so this assumption was not considered unreasonable. It was also assumed that a point source of neutrons was located at the center of the reactor. This point source is treated as a boundary condition in the following mathematical development.

In the case of finite cylindrical geometry the diffusion equation can be written

$$- D\nabla^2\phi(\rho,z) + \Sigma_a\phi(\rho,z) = S(\rho,z)$$

where $S(\rho,z) = \nu\Sigma_f\phi(\rho,z)$ for a multiplying medium and is zero for a nonmultiplying medium. Σ_f is the macroscopic fission cross section for the medium and ν is the average number of neutrons resulting from a single fission event.

If both a core and a reflector are involved, a diffusion equation must be written for both regions as follows:

$$D_c\nabla^2\phi_c(\rho,z) + \nu\Sigma_{f_c}\phi_c(\rho,z) - \Sigma_{a_c}\phi_c(\rho,z) = 0$$

$$D_R\nabla^2\phi_R(\rho,z) - \Sigma_{a_R}\phi_R(\rho,z) = 0$$

The solutions to these simultaneous equations must satisfy all the boundary conditions previously stated.

The above equations can also be written

$$\nabla^2\phi_c(\rho,z) + B_c^2\phi_c(\rho,z) = 0$$

and

$$\nabla^2\phi_R(\rho,z) - \kappa_R^2\phi_R(\rho,z) = 0$$

where $B_c^2 \equiv [\nu\Sigma_{f_c} - \Sigma_{a_c}]/D_c$ and $\kappa_R^2 \equiv \Sigma_{a_R}/D_R$. In neutron diffusion theory a term called diffusion length, L, is defined such that

$$L^2 \equiv \frac{D}{\Sigma_a}$$

Using this definition in the terms above gives

$$\kappa_R^2 = \frac{1}{L_R^2}$$

and
$$B_c^2 = \frac{1}{L_c^2}\left[\frac{\nu\Sigma_{f_c}}{\Sigma_{a_c}} - 1\right] = \frac{k_\infty - 1}{L_c^2}$$

where $k_\infty \equiv \nu\Sigma_{f_c}/\Sigma_{a_c}$ is the infinite multiplication constant for a medium composed of the same material as the reactor core.

In cylindrical coordinate the ∇^2 operator is

$$\nabla^2 = \frac{1}{\rho}\frac{\partial}{\partial\rho}\left[\rho\frac{\partial}{\partial\rho}\right] + \frac{\partial^2}{\partial z^2} \quad ,$$

so the above diffusion equations become

$$\frac{1}{\rho}\frac{\partial}{\partial\rho}\left[\rho\frac{\partial}{\partial\rho}\phi_c(\rho,z)\right] + \frac{\partial^2}{\partial z^2}\phi_c(\rho,z) + B_c^2\phi_c(\rho,z) = 0$$

and
$$\frac{1}{\rho}\frac{\partial}{\partial\rho}\left[\rho\frac{\partial}{\partial\rho}\phi_R(\rho,z)\right] + \frac{\partial^2}{\partial z^2}\phi_R(\rho,z) - \kappa_R^2\phi_R(\rho,z) = 0$$

both of which can be solved by the method of separation of variables.

For the core it is assumed that

$$\phi_c(\rho,z) = R_c(\rho)Z_c(z)$$

and the resultant general solutions to the separated diffusion equation for the core are, if $B_c^2 \equiv k_\rho^2 + k_z^2$,

$$Z_c(z) = A_z \sin k_z z + C_z \cos k_z z$$

$$R_c(\rho) = A_\rho J_o(k_\rho \rho) + C_\rho Y_o(k_\rho \rho)$$

where $J_o(k_\rho \rho)$ and $Y_o(k_\rho \rho)$ are zero order Bessel functions of the first and second kinds, respectively. The function $Y_o(k_\rho \rho)$, which approaches negative infinity as ρ approaches the value of zero, becomes more negative for small values of $(k_\rho \rho)$ than the function $J_o(k_\rho \rho)$ becomes positive. Thus since the boundary conditions stipulate that $\phi(\rho,z)$ can never be negative, C_ρ must be taken to be zero. Since $\sin k_z z$ becomes negative when z becomes negative, this term would violate the physical requirement that $\phi(\rho,z)$ be symmetric about the $z = 0$ plane. Thus, A_z must also be taken to be zero.

Hence, the solution for the core region is

$$\phi_c(\rho,z) = A_c J_o(k_\rho \rho) \cos k_z z \ .$$

For the reflector it is also assumed that

$$\phi_R(\rho,z) = R_R(\rho)Z_R(z)$$

and the resultant general solutions to the separated diffusion equation for the reflector are, if $\kappa_R^2 \equiv \kappa_\rho^2 - \kappa_z^2$,

$$Z_R(z) = A_z \sin \kappa_z z + C_z \cos \kappa_z z$$

$$R_R(\rho) = A_\rho I_o(\kappa_\rho \rho) + C_\rho K_o(\kappa_\rho \rho)$$

where $I_o(\kappa_\rho \rho)$ and $K_o(\kappa_\rho \rho)$ are zero order modified Bessel functions of the first and second kinds, respectively. Here again, the condition of symmetry of the neutron flux about $z = 0$ requires that A_z be taken to be zero.

Hence, the solution for the reflector region is

$$\phi_R(\rho,z) = [A_R I_o(\kappa_\rho \rho) + C_R K_o(\kappa_\rho \rho)] \cos \kappa_z z \ .$$

If ρ_o and z_o are defined to be the extrapolated radius and height, then the flux must be zero at the points where $\rho = \rho_o$ or where $z = z_o$. This boundary condition requires that $\phi_R(\rho,z) = 0$ when $\rho = \rho_o$ or when $z = z_o$. So $\kappa_z z_o = \pi/2$ since $\cos \pi/2 = 0$. Thus $\kappa_z = \pi/2z_o$.

This boundary condition also requires that

$$[A_R I_o(\kappa_\rho \rho) + C_R K_o(\kappa_\rho \rho)] = 0 \quad \text{when } \rho = \rho_o.$$

Thus

$$A_R = - C_R \frac{K_o(\kappa_\rho \rho_o)}{I_o(\kappa_\rho \rho_o)}$$

The equations for the flux in the reactor thus become, in summary,

$$\phi_c(\rho,z) = A_c J_o(k_\rho \rho) \cos k_z z$$

$$\phi_R(\rho,z) = C_R \left[K_o(\kappa_\rho \rho) - \frac{K_o(\kappa_\rho \rho_o)}{I_o(\kappa_\rho \rho_o)} I_o(\kappa_\rho \rho) \right] \cos \frac{\pi}{2 z_o} z$$

where z_o and ρ_o are the extrapolated height and radius, respectively.

At the interface between the core and the reflector, the boundary conditions require that the flux and the net current be continuous across the interface. Since the current is a vector quantity, this condition requires that the components of the current vectors be continuous. Thus, at the interface denoted by height z_i and radius ρ,

$$\phi_c(\rho,z_i) = \phi_R(\rho,z_i)$$

and

$$J_{c_z}(\rho,z_i) = J_{R_z}(\rho,z_i)$$

which leads to the equations

$$A_cJ_o(k_\rho\rho)\cos k_zz_i = C_R\left[K_o(\kappa_\rho\rho) - \frac{K_o(\kappa_\rho\rho_o)}{I_o(\kappa_\rho\rho_o)} I_o(\kappa_\rho\rho)\right]\cos\frac{\pi}{2z_o} z_i$$

and

$$D_ck_zA_cJ_o(k_\rho\rho)\sin k_zz_i$$

$$= \frac{\pi}{2z_o} D_RC_R\left[K_o(\kappa_\rho\rho)-\frac{K_o(\kappa_\rho\rho_o)}{I_o(\kappa_\rho\rho_o)} I_o(\kappa_\rho\rho)\right]\sin\frac{\pi}{2z_o} z_i .$$

Dividing the second of these equations by the first gives the equation

$$k_z \tan k_zz_i = \frac{\pi}{2z_o}\frac{D_R}{D_c}\tan\frac{\pi}{2z_o} z_i ,$$

which can be solved by numerical methods to determine k_z after the values of D_R, D_c, z_i , and z_o are computed or measured for the reactor being studied.

Once the values for k_z and κ_z are known, the corresponding values of k_ρ and κ_ρ can be computed from the relations

$$B_c^2 = k_\rho^2 + k_z^2 \qquad \text{and} \qquad \kappa_R^2 = \kappa_\rho^2 - \kappa_z^2$$

since B_c^2 and κ_R^2 depend on the physical constants of the reactor and these constants are known.

The constant A_c is related to the constant C_R by the interface boundary condition that the flux must be continuous at the interface denoted by radius ρ_i and the height z. Thus $\phi_c(\rho_i,z) = \phi_R(\rho_i,z)$ or, if the point where $z = 0$ is taken,

$$C_R = A_c \frac{J_o(k_\rho \rho_i)}{\left[K_o(\kappa_p \rho_i) - \frac{K_o(\kappa_\rho \rho_o)}{I_o(\kappa_\rho \rho_o)} I_o(\kappa_\rho \rho_i)\right]}$$

which will give C_R as a constant multiplied by A_c.

The constant A_c can be evaluated by the boundary condition of continuity of net neutron current at the interface between the external neutron source and the core. If comparison of theory with experimentally determined flux distributions is desired, then the maximum value of the flux can be used for A_c.

The values of D_c, D_R, B_c, k_ρ, k_z, κ_R, κ_ρ, κ_z, and C_R for the reactor used in this experiment are computed in Appendix A.

If the neutron density distribution, $n(\rho,z)$, rather than the flux distribution, $\phi(\rho,z)$, is desired, the the constants A_c and C_R are simply divided by the thermal

neutron velocity (220,000 cm/sec) to obtain the equations

$$n_c(\rho,z) = A_c'J_o(k_\rho \rho) \cos k_z z$$

$$n_R(\rho,z) = C_R'\left[K_o(\kappa_\rho \rho) - \frac{K_o(\kappa_\rho \rho_o)}{I_o(\kappa_\rho \rho_o)} I_o(\kappa_\rho \rho)\right] \cos \kappa_z z$$

where $A_c' = A_c/v_{th}$ and $C_R' = C_R/v_{th}$.

B. One Velocity Group Diffusion Theory Approximation with Control Rods[2]

Since the diffusion theory differential equations are the same for the core and reflector regions regardless of the presence of a control rod, the general solutions for these equations remain the same as for the case when no control rod is present. The effect of the control rod is accounted for by the boundary conditions used to evaluate the constants.

The general solutions for the diffusion equations are

$$\phi_c(\rho,z) = [A_c J_o(k_\rho \rho) + C_c Y_o(k_\rho \rho)] \cos k_z z$$

$$\phi_R(\rho,z) = [A_R I_o(\kappa_\rho \rho) + C_R K_o(\kappa_\rho \rho)] \cos \kappa_z z$$

---

[2] R. V. Meghreblian and D. K. Holmes, Reactor Analysis (New York: McGraw-Hill Book Co., 1960), Chap. 11.

where $B_c^2 \equiv k_\rho^2 + k_z^2$ and $\kappa_R^2 \equiv \kappa_\rho^2 - \kappa_z^2$ as before, and $J_o(k_\rho \rho)$ and $Y_o(k_\rho \rho)$ are zero order Bessel functions of the first and second kinds, respectively, and $I_o(\kappa_\rho \rho)$ and $K_o(\kappa_\rho \rho)$ are zero order modified Bessel functions of the first and second kinds, respectively.

The boundary conditions which were applicable for the case with no control rod remain applicable, and for the case of a black control rod fully inserted along the axis of a cylindrical reactor, the additional boundary condition that $\phi_c = 0$ at the point where $\rho = b_o$ must be imposed. The radius b_o is defined by the relation

$$b_o = b - \epsilon$$

where b is the radius of the control rod and ϵ is the extrapolation distance into the rod.

When a black control rod is present, the flux becomes zero for $\rho > 0$, and so the term $Y_o(k_\rho \rho)$ need not be eliminated from the equation for $\phi_c(\rho, z)$. The boundary condition that $\phi_c(b_o, z) = 0$ yields the relationship

$$A_c J_o(k_\rho b_o) = - C_c Y_o(k_\rho b_o).$$

This relation can be used to eliminate C_c and yield the

equation

$$\phi_c(\rho,z) = A_c\left[J_o(k_\rho\rho) - \frac{J_o(k_\rho b_o)}{Y_o(k_\rho b_o)}\,Y_o(k_\rho\rho)\right]\cos k_z z\ ,$$

where A_c, k_ρ, and k_z are yet to be determined.

The boundary condition that $\phi_R(\rho,z) = 0$ at the extrapolated radius, ρ_o, and height, z_o, yields, as for the case of no control rod, the relationships

$$k_z = \frac{\pi}{2z_o}$$

and
$$A_R = -\,C_R\,\frac{K_o(\kappa_\rho\rho_o)}{I_o(\kappa_\rho\rho_o)}$$

where κ_ρ can be determined from the definition $\kappa_R^2 = \kappa_\rho^2 - \kappa_z^2$ when z_o is known.

In summary, the equations for the flux can now be written

$$\phi_c(\rho,z) = A_c\left[J_o(k_\rho\rho) - \frac{J_o(k_\rho b_o)}{Y_o(k_\rho b_o)}\,Y_o(k_\rho\rho)\right]\cos k_z z$$

$$\phi_R(\rho,z) = C_R\left[K_o(\kappa_\rho\rho) - \frac{K_o(\kappa_\rho\rho_o)}{I_o(\kappa_\rho\rho_o)}\,I_o(\kappa_\rho\rho)\right]\cos \kappa_z z$$

where κ_z, b_o, and κ_ρ are known.

The boundary condition for continuity of flux and net neutron current are used to determine the remaining constants.

At the interface denoted by height z_i and radius ρ, the relations

$$\phi_c(\rho, z_i) = \phi_R(\rho, z_i)$$

and

$$J_{c_z}(\rho, z_i) = J_{R_z}(\rho, z_i)$$

must be true. These relations again lead to the equation

$$\frac{\cos k_z z_i}{D_c k_z \sin k_z z_i} = \frac{\cos \kappa_z z_i}{D_R \kappa_z \sin \kappa_z z_i}$$

which can be written

$$k_z \tan k_z z_i = \frac{D_R}{D_c} \frac{\pi}{2z_o} \tan \frac{\pi}{2z_o} z_i$$

and can be solved by numerical methods in order to determine k_z. After k_z is determined, k_ρ can be found from the relation $B_c^2 = k_\rho^2 + k_z^2$, which has previously been defined.

The relationship between A_c and C_R is determined by the boundary condition that $\phi_c = \phi_R$ at the interface

denoted by radius ρ_i and height z. This condition yields the relationship

$$C_R = A_c \frac{\left[J_o(k_\rho \rho_i) - \frac{J_o(k_\rho b_o)}{Y_o(\kappa_\rho \rho_o)} Y_o(k_\rho \rho_i)\right]}{\left[K_o(\kappa_\rho \rho_i) - \frac{K_o(\kappa_\rho \rho_o)}{I_o(\kappa_\rho \rho_o)} I_o(\kappa_\rho \rho_i)\right]}$$

if the z = 0 plane is used for the evaluation.

In a similar manner, the boundary condition that $J_{c_\rho} = J_{R_\rho}$ at the interface denoted by radius ρ_i and the z = 0 plane can be used to determine A_c since this would give two simultaneous equations containing A_c and C_R. In order to correlate theory with experiment, A_c can alternatively be taken to be the flux observed along the midplane at the distance ρ for which

$$\left[J_o(k_\rho \rho) - \frac{J_o(k_\rho b_o)}{Y_o(k_\rho b_o)} Y_o(k_\rho \rho)\right] = 1 .$$

The values of all constants except A_c and C_R are the same as when no control rod was present. The values of A_c and C_R for the reactor used in this experiment are computed in Appendix A.

If the neutron density distribution, $n(\rho,z)$, is desired rather than the flux distribution, $\phi(\rho,z)$, the constants A_c and C_R are divided by the thermal neutron velocity (220,000 cm/sec) to obtain the equations

$$n_c(\rho,z) = A_c' \left[J_0(k_\rho \rho) - \frac{J_0(k_\rho b_0)}{Y_0(k_\rho b_0)} Y_0(k_\rho \rho) \right] \cos k_z z$$

$$n_R(\rho,z) = C_R' \left[K_0(\kappa_\rho \rho) - \frac{K_0(\kappa_\rho \rho_0)}{I_0(\kappa_\rho \rho_0)} I_0(\kappa_\rho \rho) \right] \cos \kappa_z z$$

where $A_c' \equiv A_c/v_{th}$ and $C_R' \equiv C_R/v_{th}$.

CHAPTER II

NEUTRON FLUX MEASUREMENT BY THE ACTIVATION METHOD

A. General

The activation method provides one of the most convenient and most accurate techniques for measuring neutron flux. This method is based on the fact that many elements become radioactive when exposed to a neutron flux. For several elements, this activation occurs only for a narrow range of neutron energies. By measurement of the induced activity, the neutron flux responsible for the activation can be determined.

To measure a flux, a thin foil of the most suitable material is first irradiated for a certain time interval at the desired location. The foil is then removed from the neutron flux and the induced activity is measured in an appropriate counting device. The relationship between the measured activity and the neutron flux must include correction terms for such things as counter efficiency and depression of neutron flux by the foil being used to perform the measurement.

In order to be suitable for this type of measurement, the foil material should have a large neutron absorption cross section for the energy range to be studied. Also, the decay scheme of the radioactive isotope produced by the neutron activation should be simple enough for easy measurement and interpretation, and the half life for decay of this product isotope should be such that irradiation and counting periods are not excessively long.

For thermal neutron detection, the most frequently used elements[3] which have strong resonance absorptions and yield induced radioactivity of suitable half lives and radiations are In, Rh, Ag. Au, I, and Dy.

B. Use of Dysprosium Foils for Thermal Neutron Detection

The dimensions of the subcritical reactor used in this project made necessary the use of a Van de Graaff accelerator to produce the external source of neutrons necessary for a subcritical reactor (see Chapter III). Due to the operational characteristics of the accelerator used, it was possible to maintain a constant source strength for only

---

[3] C. F. Bonilla, Nuclear Engineering (New York: McGraw-Hill Book Co., Inc., 1957), p. 129.

short periods of time, and, hence, the foil detector material used had to be such that maximum induced activity could be reached in the shortest period of time feasible. Of the foil materials (In, Au, and Dy) available, dysprosium, which has a large cross section for thermal neutron absorption as well as a low cross section for epithermal neutron absorption, best met this requirement. However, dysprosium does have one disadvantage in that approximately twenty hours must be allowed for adequate decay of the induced activity prior to reusing a particular foil for another measurement.

Preliminary calculations showed that, of the several naturally occurring isotopes of dysprosium which could result in radioactive products when irradiated by neutrons, only the isotope Dy^{164} need be considered. Contributions to induced activity from neutron absorption by isotopes Dy^{156} and Dy^{158} are negligible due to low percentages of abundance and small neutron absorption cross sections as well as the long half life of decay of the radioactive products Dy^{157} and Dy^{159}. The contribution to measurable activity by the transformation of Dy^{165} into the radioactive isotope Dy^{166} was determined by calculation to be less than 2×10^{-14} per cent. These calculations were confirmed by

experimental determination of the half life of decay for the activity induced in natural dysprosium by neutron activation. The observed half life was exactly that of Dy^{165}.

Thus, only the activity induced through neutron absorption by the isotope Dy^{164} need be considered in connection with neutron flux measurements. The reactions involved are:

$$Dy^{164} + n \rightarrow Dy^{165m} \begin{array}{l} \nearrow \; Dy^{165} + \gamma \\ \\ \searrow \; Ho^{165} + \beta^{-} + \gamma \end{array}$$

$$Dy^{164} + n \rightarrow Dy^{165} \rightarrow Ho^{165} + \beta^{-} + \gamma$$

The decay scheme for Dy^{165} is shown in Figure II-1.

The general differential equation for formation of radioactive product nuclei by the neutron absorption reaction is, in word form,

$$\left[\begin{array}{l}\text{Rate of accumula-}\\ \text{tion of radio-}\\ \text{active nuclei}\end{array}\right] = \left[\begin{array}{l}\text{Rate of produc-}\\ \text{tion of radio-}\\ \text{active nuclei}\end{array}\right] - \left[\begin{array}{l}\text{Rate of loss}\\ \text{of radio-}\\ \text{active nuclei}\end{array}\right]$$

In the case of Dy^{164} two differential equations are necessary since Dy^{164} can be transformed into both Dy^{165} and

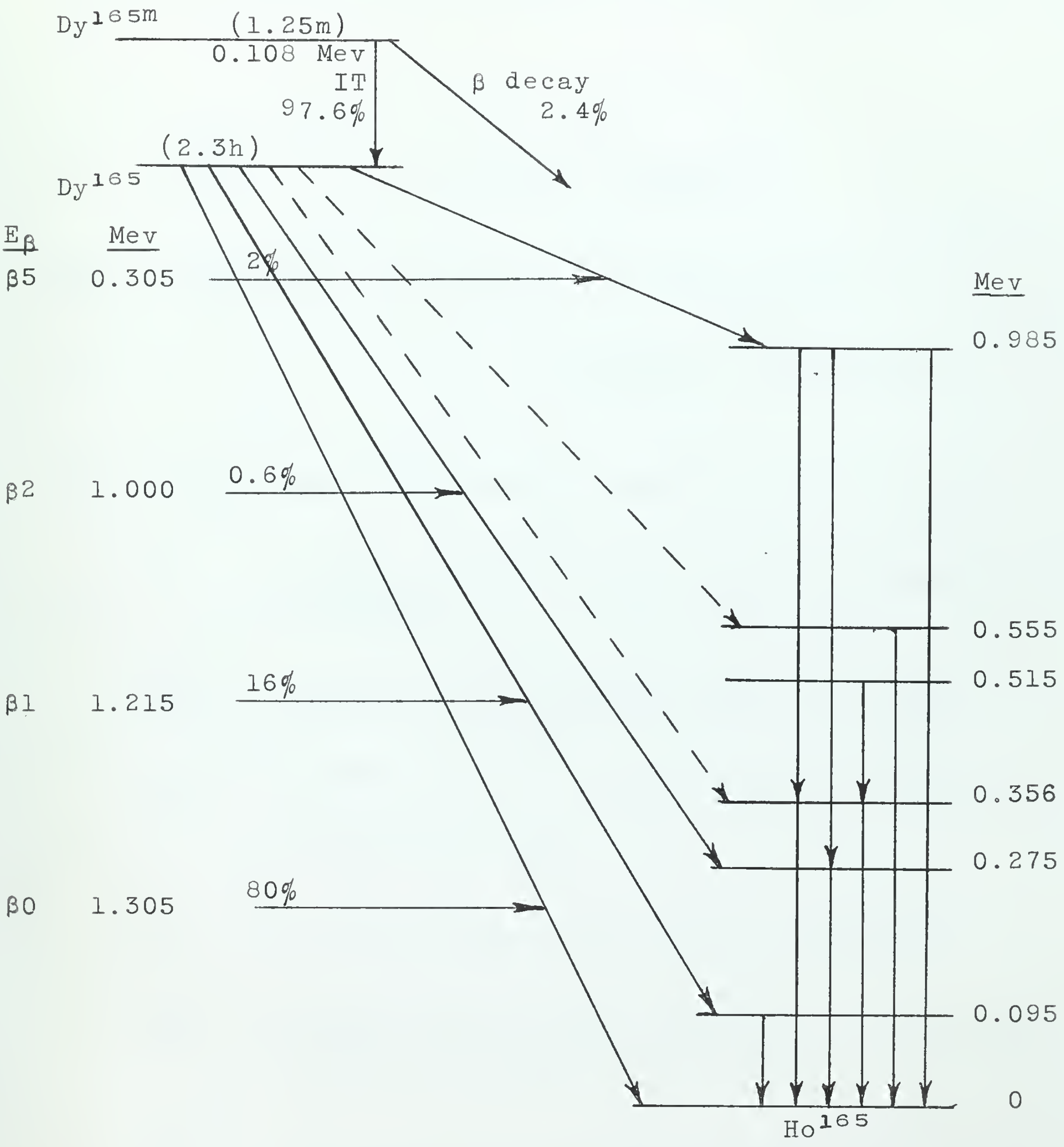

Figure II-1. Decay Scheme for Dy^{165} (from Tornau*)

---

*Rüdiger Tornau, Zeitschrift für Physik, 159, p. 101, 1960.

Dy^{165m} by the neutron absorption reaction. These equations are:

$$(1) \qquad \frac{d\,D_{5m}(T)}{dT} = \sigma_{n\gamma}^{4-5m} D_4 \phi_{th} - \lambda_{5m} D_{5m}(T)$$

$$(2) \qquad \frac{d\,D_5(T)}{dT} = \sigma_{n\gamma}^{4-5} D_4 \phi_{th} + 0.976\,\lambda_{5m} D_{5m}(T) - \lambda_5 D_5(T) - \sigma_{n\gamma}^{5-6} D_5(T) \phi_{th}$$

The notation used in the above equations is as follows:

D_4 = number of Dy^{164} nuclei present (assumed to be constant)

$D_5(T)$ = number of Dy^{165} nuclei present at time T.

$D_{5m}(T)$ = number of Dy^{165m} nuclei present at time T.

T = irradiation time

ϕ_{th} = thermal neutron flux during irradiation

$\sigma_{n\gamma}^{4-5}$ = thermal neutron absorption cross section for activation of Dy^{164} to Dy^{165}.

$\sigma_{n\gamma}^{4-5m}$ = thermal neutron absorption cross section for activation of Dy^{164} to Dy^{165m}.

$\sigma_{n\gamma}^{5-6}$ = thermal neutron absorption cross section for activation of Dy^{165} to Dy^{166}.

λ_5 = decay constant for Dy^{165}.

λ_{5m} = decay constant for Dy^{165m}.

Preliminary calculations showed that the effect of the activation of Dy^{165} to Dy^{166} is completely negligible, so the solutions to these two simultaneous differential equations are found, by standard methods, to be

$$D_{5m}(T) = \frac{\sigma_{n\gamma}^{4-5m} D_4 \phi_{th}}{\lambda_{5m}} \left[1 - \exp(-\lambda 5mT) \right]$$

and $$D_5(T) = B\left[1 - \exp(-\lambda_5 T)\right] + C\left[\exp(-\lambda_{5m}T) - \exp(-\lambda_5 T)\right]$$

where $$B \equiv \frac{\sigma_{n\gamma}^{4-5} D_4 + 0.976\ \sigma_{n\gamma}^{4-5m} D_4}{\lambda_5} \phi th$$

and $$C \equiv \frac{0.976\ \sigma_{n\gamma}^{4-5m} D_4}{(\lambda_{5m} - \lambda_5)} \phi th .$$

In determining these solutions the boundary condition that both $D_5(T)$ and $D_{5m}(T)$ were zero at time $T = 0$ was used.

If the foil is removed from the neutron flux at time T, the number of Dy^{165} and Dy^{165m} nuclei present at any time t thereafter is determined by the solutions to the differential equations

$$\frac{dD_{5m}(t)}{dt} = - \lambda_{5m} D_{5m}(t)$$

and $$\frac{dD_5(t)}{dt} = 0.976\ \lambda_{5m} D_{5m}(t) - \lambda_5 D_5(t) .$$

In this case the boundary conditions to be used are that $D_{5m}(t) = D_{5m}(T)$ and $D_5(t) = D_5(T)$ at $t = 0$, where t is time after removal from the neutron flux.

The solutions to these simultaneous differential equations are

$$D_{5m}(t) = D_{5m}(T) \left[\exp\ (-\lambda_{5m} t) \right]$$

and $$D_5(t) = \frac{0.976\ \lambda_{5m}}{(\lambda_5 - \lambda_{5m})} D_{5m}(T) \left[\exp\ (-\lambda_{5m} t) - \exp\ (-\lambda_5 t) \right]$$

$$+ D_5(T) \left[\exp\ (-\lambda_5 t) \right].$$

Since the activity at any time t is simply the product of the decay constant and the number of nuclei present at that time, the following equations give the activity as a function of the time after removal of the detector foil from the neutron flux:

$$A_{5m}(t) = \lambda_{5m} D_{5m}(t)$$

$$A_5(t) = \lambda_5 D_5(t)$$

Thus, if the activity is counted for a specific time interval, t_1 to t_2, the number of radioactive disintegrations, N, occurring during this time will be

$$N = \int_{t_1}^{t_2} A_{5m}(t)\, dt + \int_{t_1}^{t_2} A_5(t)\, dt$$

$$= \int_{t_1}^{t_2} \lambda_{5m} D_{5m}(t)\, dt + \int_{t_1}^{t_2} \lambda_5 D_5(t)\, dt$$

where N = total number of disintegrations occurring between times t_1 and t_2. Evaluation of this integral yields

$$N = \left[D_5(T) - \frac{0.976\ \lambda_{5m}}{(\lambda_5 - \lambda_{5m})} D_{5m}(T) \right] \left[\exp\ (-\ \lambda_5 t_1) - \exp\ (-\ \lambda_5 t_2) \right]$$

$$+ \left[\frac{1.976\ \lambda_5 - \lambda_{5m}}{(\lambda_5 - \lambda_{5m})} D_{5m}(T) \right] \left[\exp\ (-\lambda_{5m} t_1) - \exp\ (-\ \lambda_{5m} t_2) \right]$$

This equation for N appears to be extremely cumbersome and unwieldy, but after the constants are evaluated and the time intervals to be used for irradiation and counting are decided upon, the above equation reduces to N = constant × m ϕ_{th} where m is the weight of the detector foil in grams.

Trial runs and calculations using foils of various weights indicated that an irradiation time of five minutes ($T = 0$ to $T = 5$) and a counting interval of 10 minutes ($t_1 = 15$ to $t_2 = 25$) would give very accurate results. Evaluation of the various constants needed for the above equations was carried out and the results are tabulated in Table II-1. Using these constants, the equation for N reduces to

$$N = 0.6402\ m\phi_{th}$$

where m = foil mass in grams and ϕ_{th} = neutron flux in neutrons per cm^2-min. After converting the flux into neutrons per square centimeter per second, the equation for thermal neutron flux can be written as follows:

$$\phi_{th}\left(\frac{\text{neutrons}}{\text{cm}^2\ \text{sec}}\right) = \frac{N}{38.412\ m(\text{grams})}$$

C. Determination of Thermal Neutron Flux from Measured Activity

The measured activity must be multiplied or divided by several correction factors in order to account for losses occurring in the counting process, according to

TABLE II-1

CONSTANTS TO BE USED IN EQUATION FOR NUMBER OF DISINTEGRATIONS DURING COUNTING INTERVAL

Cross Sections*	$\sigma_{n\gamma}^{4-5} = 800 \times 10^{-24}\mathrm{cm}^2$	$\sigma_{n\gamma}^{4-5m} = 2000 \times 10^{-24}\mathrm{cm}^2$
Decay Constants	$\lambda_5 = \frac{0.693}{139.2\ \mathrm{min}} = 0.004978\ \mathrm{min}^{-1}$	
	$\lambda_{5m} = \frac{0.693}{1.25\ \mathrm{min}} = 0.5544\ \mathrm{min}^{-1}$	
Product of Decay Constants and Times $\left[\begin{array}{l} T = 5\ \mathrm{min} \\ t_1 = 15\ \mathrm{min} \\ t_2 = 25\ \mathrm{min} \end{array}\right]$	$\lambda_5 T = 0.02489$	$\lambda_{5m} T = 2.7720$
	$\lambda_5 t_1 = 0.07467$	$\lambda_{5m} t_1 = 8.3160$
	$\lambda_5 t_2 = 0.12445$	$\lambda_{5m} t_2 = 13.8600$
Values of Exponentials	$e^{-\lambda_5 T} = 0.97541$	$e^{-\lambda_{5m} T} = 0.062536$
	$e^{-\lambda_5 t_1} = 0.92805$	$e^{-\lambda_{5m} t_1} = 0.000245$
	$e^{-\lambda_5 t_2} = 0.88298$	$e^{-\lambda_{5m} t_2} = 0.000001$
	$e^{-\lambda_5 t_1} - e^{-\lambda_5 t_2} = 0.04507$	
	$e^{-\lambda_{5m} t_1} - e^{-\lambda_{5m} t_2} = 0.000244$	

---

*Hughes, Magurno, and Brussel, Neutron Cross Sections, Supplement No. 1 to BNL 325, U. S. Government Printing Office, Washington 25, D. C., January 1960.

Greenfield, Koontz, Jarrett, and Taylor.[4] When the activity being counted is beta activity, losses are experienced due to self-absorption and scattering by the foil material as well as the usual losses due to counter efficiency, flux depression, geometry factor, etc.

If N is the number of disintegrations occurring during the interval in which the neutron detector foil is counted, and C_{th} is the total number of counts during this interval which are due to activity induced by thermal neutrons only, then the relationship between N and C_{th} is

$$N = \frac{C_{th}\ F_{sp}\ (d)}{1.011\ F_{\gamma}\ F_{g}\ F_{e}\ F_{bs}\ F_{se\&sc}(d)}$$

where the factor 1.011 is a correction factor to take into account the Maxwellian distribution of thermal neutrons as well as the dependence on neutron energy of the $\sigma_{n\gamma}$ values for the detector foil material. The F factors are correction factors for gamma photon counts from competing modes of decay in dysprosium, detector geometry, counter efficiency, back scattering, self absorption and self scatter in the foil, and flux depression by the foil. The factors F_{sp} and $F_{sa\&sc}$ are dependent on the foil thickness, d.

---

[4] Greenfield, Koontz, Jarrett, and Taylor, Nucleonics, 15, No. 3, p. 57, March, 1957.

The total counts observed, C_{th}, which are due to activity induced by thermal neutrons is determined by taking one measurement, C_{cd}, in a certain location with a foil wrapped in a cadmium cover, and by taking a second measurement, C_{total}, in exactly the same location using the same foil with no cadmium cover. The difference of these measurements is the desired value, C_{th}. The mathematical expression for C_{th} is

$$C_{th} = C_{tot} - C_{cd}$$

when the foil material is dysprosium. For materials which have large resonances in their absorption cross sections for neutron energies greater than thermal, the cadmium covered foil measurement, C_{cd}, must be multiplied by a correction factor F_{cd} to account for epithermal neutrons absorbed by the cadmium cover. However, in the case of dysprosium,[5] there are no such large resonances, and thus, since C_{cd} is only about 1 per cent of C_{total}, this correction is not necessary. Preliminary data taken using dysprosium foils showed that omission of this correction factor, F_{cd}, which

---

[5] C. W. Tittle, Nucleonics, 8, No. 6, p. 5, June, 1951.

as yet has not been experimentally determined for the case when the detector foil material is dysprosium, would introduce an error of less than 0.07 per cent in the data taken for this thesis.

Since the beta counting apparatus used (see Chapter III) had 4π geometry, the correction factor for geometry, F_g, is equal to unity. The scintillator container dimensions were such that all beta particles were captured prior to their reaching the walls of the container. Thus, the correction factor for back scattering, F_{bs}, is also equal to unity.

All gamma rays emitted during the 10-minute counting interval are coincidental with the beta particles which are being counted, so the factor F_γ, which compensates for gamma photons emitted by decay modes other than the one being measured, is also equal to unity. The 15-minute waiting period prior to the counting interval was purposely chosen so that the number of gamma rays from the isomeric transition of Dy^{165m} to Dy^{165} (half life of 1.25 min.) would be completely negligible in that less than 0.025 per cent of the activity present due to this decay mode at time $t = 0$ remains at time t_1 (= 15 minutes).

The factor, F_{sp}, which compensates for the depression of the thermal neutron flux by the foils being used to conduct the measurements, can be calculated by the equation[6]

$$F_{sp}(d) = 1 + \frac{0.34\ \alpha R}{\lambda_{tr}} \text{ if } R << \lambda_{tr}$$

which was developed by Bothe. In this equation R = foil radius and $\lambda_{tr} = \frac{\lambda_s}{1 + (\cos\ \theta)_{avg}}$ = the transport mean free path in the reactor. λ_s is the scattering mean free path in the reactor, and $(\cos\ \theta)_{avg} = 2/3A$ where A is the mass number of the scattering nucleus. The term α depends on the foil thickness, d, and is determined by the equation

$$\alpha(d) = 1 - \left[\exp\ (-\ \mu d)\right](1 - \mu d) + \mu^2 d^2 E_i(-\mu d)$$

where d is thickness of the detector foil, μ is the thermal neutron absorption coefficient for this foil, and $E_i\ (-\mu d)$ is the exponential integral function[7] value for the foil.

---

[6] C. W. Tittle, Nucleonics, 9, No. 1, p. 60, July, 1951.

[7] E. Jahnke, and F. Emde, Tables of Functions, Dover Pub. Co., New York, 1943.

Calculations using this equation were compared with experimental values by Bothe,[8] and agreement was excellent even for cases where the foil radius, R, was only slightly less than λ_{tr}. Thus this equation was used to calculate $F_{sp}(d)$ for the foils used in this project. The values calculated are tabulated in Chapter IV.

The factor F_e accounts for the efficiency of the beta detection apparatus and is less than unity even for a 4π geometry detector since the contributions by low energy beta particles may be lost in the tube noise (see Chapter III). The factor $F_{sa\&sc}(d)$, the correction for self absorption and self scattering of beta particles by the foil, is dependent on foil thickness and has not been determined for dysprosium foils. By coincidence measurements utilizing the fact that gamma rays are emitted simultaneously with beta particles in the decay of Dy^{165}, the combined correction factor $\left[F_e\ F_{sa\&sc}(d)\right]$ can be determined. The equations used in this determination are:

$C_\gamma = Kf_e f_g N$ For the gamma ray counter

$C_\beta = F_e F_{sa\&sc} F_g\ N$ For the beta particle counter

---

[8] C. W. Tittle, Nucleonics, 9, No. 1, p. 60, July, 1951.

and $C_{\beta-\gamma} = K f_e f_g F_e F_{sa\&sc} N$ for the coincidence counter where N = number of Dy^{165} disintegrations during the counting interval and the C's are the various observed counts corrected for background. The factor $[K\ f_e\ f_g]$ accounts for the geometry and efficiency of the gamma detector and for gamma rays absorbed prior to reaching the gamma ray detector. Elimination of $[K\ f_e\ f_g]$ yields the equation, since F_g is known to be unity, $N = C_\beta C_\gamma / C_{\beta-\gamma}$. Thus, if C_β for the 4π counter is then measured,

$$\frac{C_\beta(4\pi \text{ counter})}{N} = F_e\ F_{sa\&sc} = \frac{C_{\beta-\gamma} C_\beta(4\pi \text{ counter})}{C_\gamma C_\beta} .$$

Since $F_{sa\&sc}$ is a function of foil thickness, d, coincidence counting measurements were conducted (see Chapter III) for each foil, and the resulting values for $[F_e\ F_{sa\&sc}(d)]$ are tabulated in Chapter IV.

Thus, when all correction factors are included, the final equation for absolute thermal neutron flux for a given number of counts observed during the counting interval t_1 (= 15 minutes) to t_2 (= 25 minutes) is given by the equation

$$\phi_{th} = \frac{[C_{total} - C_{cd}]\ F_{sp}(d)}{[1.011\ F_e\ F_{sa\&sc}(d)][38.412\ m]}$$

where m is the foil weight in grams and ϕ_{th} is in neutrons per square centimeter per second.

If the result is desired in terms of neutron density, n (neutrons/cm^3), we must divide ϕ_{th} by the thermal neutron velocity of 220,000 centimeters per second to get the equation

$$n = \frac{[C_{total} - C_{cd}]\ F_{sp}(d)}{220{,}000\ [1.011\ F_e\ F_{sa\&sc}(d)][38.412\ m]}$$

where n is in neutrons per cubic centimeter and m is the foil weight in grams.

CHAPTER III

EXPERIMENTAL APPARATUS AND PROCEDURE

A. Reactor and External Neutron Source

The University of Texas subcritical reactor[9] is composed of a polyethylene-clad, homogeneous core of 20 per cent enriched UO_2 dispersed in high strength Marlex-50 polyethylene, and three separate reflector assemblies. The core is a cylinder approximately 10 inches in diameter and approximately 14 inches long, assembled from eight homogeneous polyethylene discs impregnated with UO_2. One radial and one axial hole of approximately 1 inch diameter penetrate the core for the purpose of insertion of foils, neutron sources, etc.

The reflector assemblies are made of polyethylene and graphite. The polyethylene reflector is composed of two concentric shells, each approximately three inches thick, so that a total reflector thickness of either three

---

[9] F. D. Eichenbaum, Lockheed Nuclear Products Reports NR 57 and 58, March, 1959, Nuclear Products Division of Lockheed Aircraft Corp., Marietta, Georgia.

or six inches may be used. The graphite reflector is approximately ten inches thick. All three assemblies are constructed in the form of annular cylinders with end plugs to fill the annulus so that the core can be completely reflected.

During experimentation, the core is inserted into one of the reflector shells and the appropriate plug is inserted into the end gap, thus providing a uniform thickness of reflector at the ends and around the core. When the core is properly positioned, its axial and radial ports are aligned with similar ports provided in the reflector. Thus foils, control rods, and neutron sources, appropriate to the experiment being conducted, can be positioned in the ports.

Small, cylindrical plugs, some composed of core material and some of reflector material, are provided in sufficient quantity for filling, as appropriate to the experiment being conducted, the voids created in the reactor by the radial and axial access ports.

In this experiment the 6 inch polyethylene reflector was used. A cross sectional view of the core with the 6 inch polyethylene reflector in place is shown in Figure III-1. The dimensions in this figure are in

centimeters and are accurate dimensions rather than the approximate figures used in the above description. Dimensions of the individual core element discs as well as the various constants applicable to the core and the reflector are tabulated in Appendix A.

The cadmium control rod used in this experiment was a hollow cylindrical tube 86.2 centimeters long composed of commercially pure cadmium. This tube had an outside diameter of 2.62 centimeters and a tube wall thickness of 0.09 centimeters.

The boron control rod was a hollow cylindrical tube 80.4 centimeters long composed of polyethylene 4 per cent impregnated with boron. The outside diameter of the tube was 2.71 centimeters and the tube wall thickness was 0.13 centimeters.

Because the University of Texas Subcritical Reactor is subcritical, an external source of neutrons must be used in order to maintain a thermal neutron flux within the reactor under steady state conditions. Several manufactured Pu-Be sources with a constant neutron yield are available for use with the reactor. Unfortunately, however, the dimensions of these "fixed" sources prohibit their use inside the reactor when one of the control rods

is positioned in the axial hole. Thus, it was necessary to use the Van de Graaff accelerator to create the necessary external neutron source.

The Van de Graaff particle accelerator available for use in connection with this experiment was manufactured by High Voltage Engineering Corporation and is capable of producing deuterons accelerated to energies of up to 1 Mev. A beryllium target was bombarded by 1 Mev deuterons from the accelerator and neutrons were produced by the $Be^9(d,n)B^{10}$ reaction. The location of this external neutron source within the reactor is shown in Figure III-1.

Beryllium was chosen as the target material because the stability characteristics of the accelerator required operation at deuteron energies between 0.8 and 1.0 Mev, and, in this deuteron energy range, the $Be^9(d,n)B^{10}$ reaction afforded a better neutron yield than does any other $X(d,n)Y$ reaction. Also, since beryllium targets were available in metal disc form, the problems associated with target cooling and handling were greatly simplified by use of beryllium rather than tritium, the only other target material immediately available for use in connection with this experiment. Target cooling was accomplished by means of a stream of air blown directly on the target assembly.

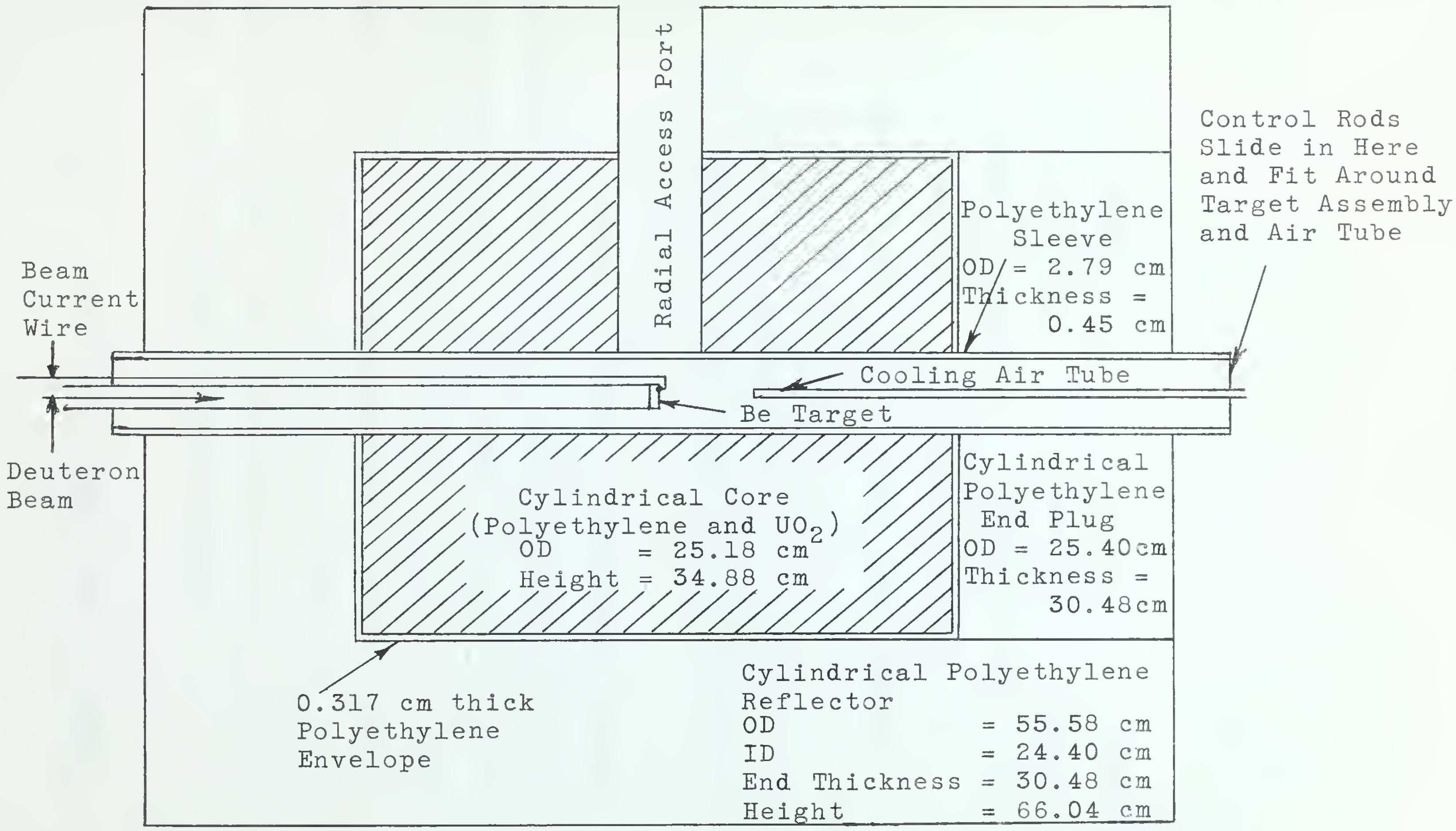

Figure III-1. Reactor Arrangement and Dimensions (Including location of external source).

The energy distribution of neutrons from the $Be^9(d,n)B^{10}$ reaction for 1 Mev deuterons (as shown in Figure III-2) shows a preponderance of neutrons having energies of approximately 3.9 Mev and 4.7 Mev. The angular distribution[10] curves for the neutrons produced by this reaction indicate only slight directional preferences, and measurements conducted to determine the strength of the source used in this experiment showed that, if an isotropic neutron yield were assumed, the maximum deviation due to directional preference would be less than 6.5 per cent. Thus, it was assumed for the purpose of this experiment that the $Be^9(d,n)B^{10}$ reaction functioned as an isotropic source of neutrons.

For this experiment, the source strength had to be determined as a function of the electrical current created by the action of the beam of accelerated deuterons produced by the accelerator and striking the beryllium target. This was accomplished by measuring with a "long counter" the number of neutrons produced at various beam current settings. These measurements were taken at various angles relative to the deuteron beam.

---

[10] A. I. Shpetnyi, Soviet Physics JETP, 5, p. 357, October, 1957.

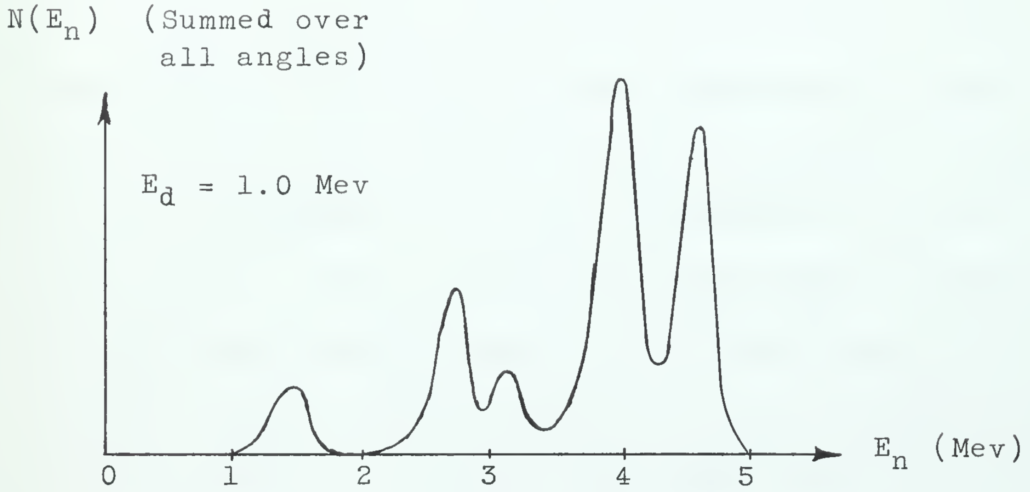

Figure III-2. Energy Distribution of Neutrons from $Be^9(d,n)B^{10}$ Reaction.--From Shpetnyi.*

---

*A. I. Shpetnyi, Soviet Physics JETP, 5, p. 357, October, 1957.

A calibrated Pu-Be isotropic neutron source with a yield of 3.5×10^6 neutrons per second was then placed in the same location that the beryllium target assembly previously occupied and the neutrons from this "known" source were counted for the same time interval using the long counter. The average of the measurements taken at various angles using the $Be^9(d,n)B^{10}$ source was assumed to be the measurement due to an "equivalent isotropic" neutron source. This average value was then divided by the measurement taken using the calibrated source and the resultant quotient was multiplied by the strength of the calibrated source in order to determine the $Be^9(d,n)B^{10}$ source strength in neutrons per second. Thus, the "equivalent isotropic" source strength for various deuteron beam currents was determined. The results are shown graphically in Figure III-3. The source strength for a beam current of 1.5 microamperes was found to be 92.2×10^6 neutrons per second.

B. Foils

As previously mentioned in Chapter II, the inherent operating characteristics of the Van de Graaff accelerator used to create the external neutron source

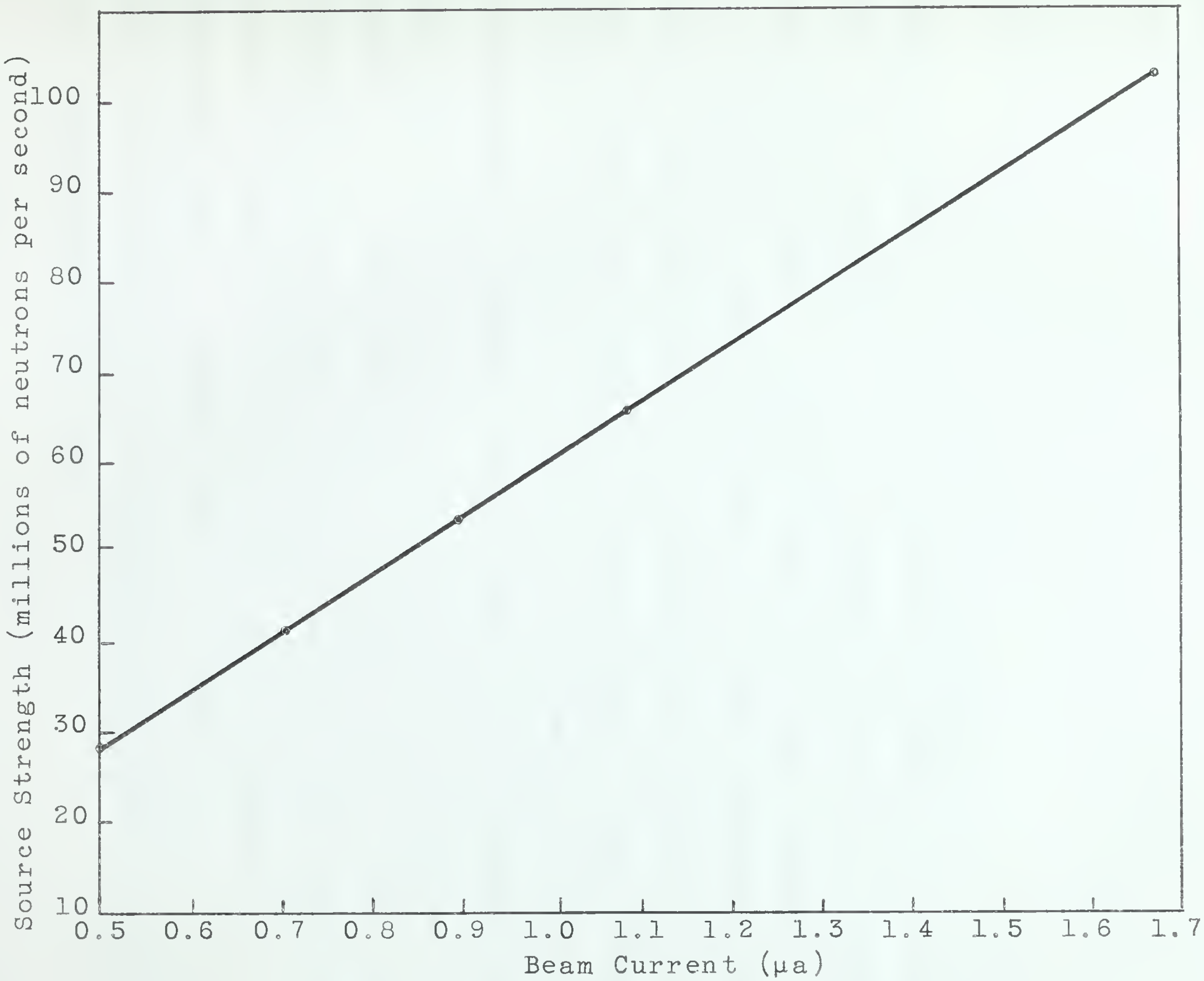

Figure III-3. Curve for "Equivalent Isotropic" Source Strength versus Deuteron Beam Current for $Be^9(d,n)B^{10}$ Reaction Using 1 Mev Deuterons.

dictated the use of dysprosium for the neutron detection material. The stable Dy^{164} isotope useful in this experiment comprises 28.2 per cent of natural dysprosium. The other isotopes contribute essentially nothing to the activity measured during this project.

Since no information concerning the self-absorption characteristics of dysprosium could be found in the literature, the variation of beta counting rate with foil thickness was determined experimentally following standard procedures.[11] Dysprosium foils of several different thicknesses were irradiated in the subcritical reactor at the same location for identical time intervals. After irradiation of each foil, 15 minutes were allowed to elapse prior to counting so that the activity due to Dy^{165m} would vanish. Each foil was then counted for a period of 10 minutes. The results are shown graphically in Figure III-4. This self-absorption curve shows a broad maximum for foil thickness between 90 mg/cm^2 and 130 mg/cm^2. This corresponds to thickness between 0.0055 inches and 0.0065 inches, so the foils were fabricated with thicknesses as close as possible to 6 thousandths of an inch.

---

[11] C. W. Tittle, Nucleonics, 8, No. 6, p. 5, June, 1951.

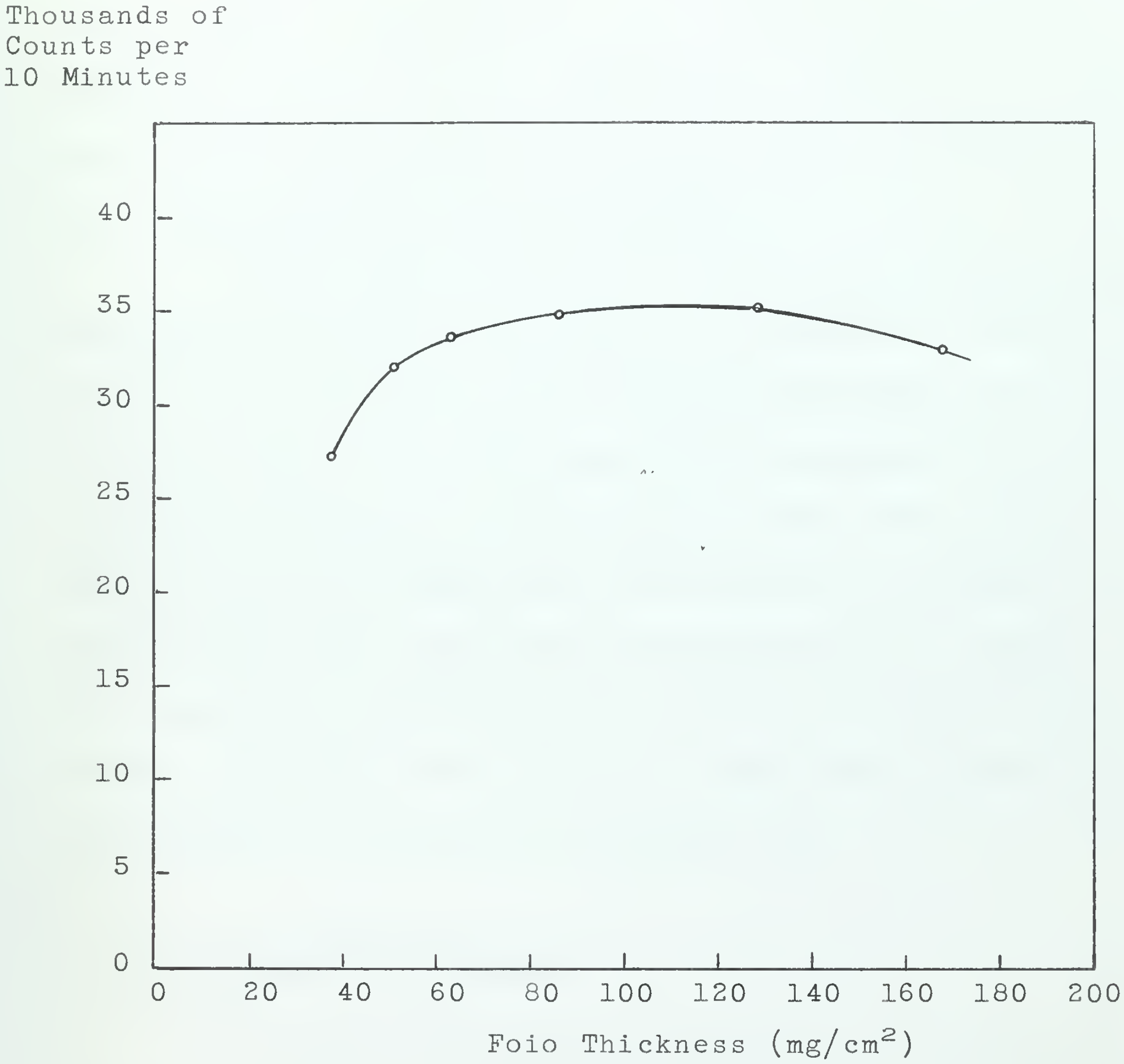

Figure III-4. Variation of Beta Counting Rate with Foil Thickness for Dysprosium Foils 1.93 cm in Diameter.

The foils used in this experiment were fabricated from a sheet of commercially pure natural dysprosium metal. Pieces of the metal were turned between centers on a lathe to a diameter of 1 centimeter and were then ground by hand to a thickness of about 6 thousandths of an inch.

Upon completion of the cutting and grinding, the foils were measured as accurately as possible. The foil weight was measured on a Wm. Ainsworth and Sons arm balance to an accuracy of 0.1 milligram. The diameters were determined by averaging five measurements taken with a microscope designed for measuring tracks made by particles in nuclear emulsions. The area was then computed, and the foil thickness was determined in units of milligrams per square centimeter. The results of these measurements and calculations are tabulated in Chapter IV.

C. Beta Counting Equipment

A liquid scintillator, composed of 4 grams per liter p-terphenyl and 0.1 gram per liter "Popop" dissolved in toluene, was used in order to create 4π geometry for beta detection.[12] This scintillator was contained in a

---

[12] T. T. Doss, Unpublished Thesis, University of Texas, June, 1961.

cylindrical aluminum sleeve with a removable aluminum cover. This sleeve (see Figure III-5) screwed into a machined brass sleeve which covered the 6810-A photomultiplier tube used to detect the scintillations created by passage of beta particles through the liquid scintillator.

Two teflon "O" rings were used to create a seal between the photomultiplier tube and the aluminum sleeve, thus holding the liquid scintillator in the upper chamber. The removable cover, which provided easy access to the liquid scintillator, had to be designed so that the system was entirely light tight when closed. This was accomplished by means of a concentric series of "tongues and grooves" machined in the surfaces of the aluminum sleeve and the cover. The foils were suspended in the liquid scintillator by means of a small spring clip attached to the removable cover.

The dimensions of the aluminum sleeve were such that the amount of liquid scintillator surrounding the foil was sufficient to absorb all the beta particles emitted by Dy^{165} decay. The maximum range of the most energetic (1.3 Mev) beta particle emitted by Dy^{165} was determined by the equation[13]

---

[13] S. Glasstone, Sourcebook on Atomic Energy (2d ed., Princeton, N.J.: D. Van Nostrand Co., 1958), p. 187.

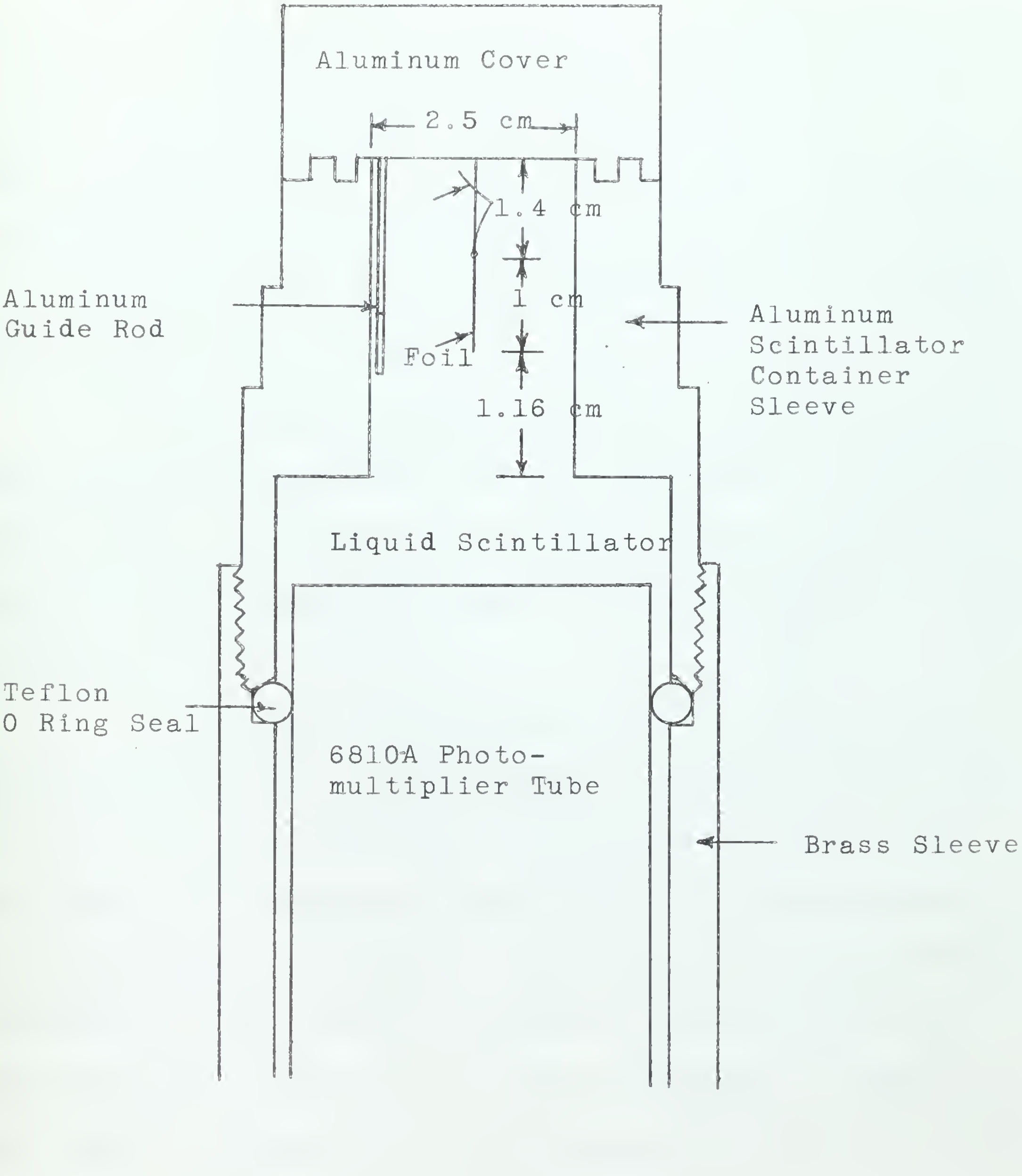

Figure III-5. Details of 4π Geometry Liquid Scintillator Beta Detector.

$$R_{max}(g/cm^2) = \frac{E_{max} - 0.17}{1.9} \text{ for } 0.5 \text{ Mev} < E_{max} < 3 \text{ Mev}$$

For E_{max} = 1.3 Mev, this equation gave a maximum range of 0.595 g/cm^2. Toluene has a density of 0.866 g/cm^3, so R_{max} was 0.688 cm in the liquid scintillator. The smallest thickness of scintillator adjacent to the foil was 0.750 cm, so all beta particles were absorbed prior to reaching the walls of the container.

The 6810A photomultiplier tube was mounted in a Texas Nuclear Corporation tube base utilizing a 417A cathode follower. A block diagram of the entire beta detecting and counting apparatus used in this experiment is shown in Figure III-6.

The proper discriminator setting for the Baird-Atomic amplifier was determined by increasing the setting from zero to the point where the observed counting rate approached the background level. At this discriminator setting, the photomultiplier tube electronic "noise" was eliminated. Undoubtedly, detection of many of the very low energy beta particles was also eliminated. However, this loss is corrected by the $F_eF_{sa\&sc}(d)$ factor previously discussed in Chapter II.

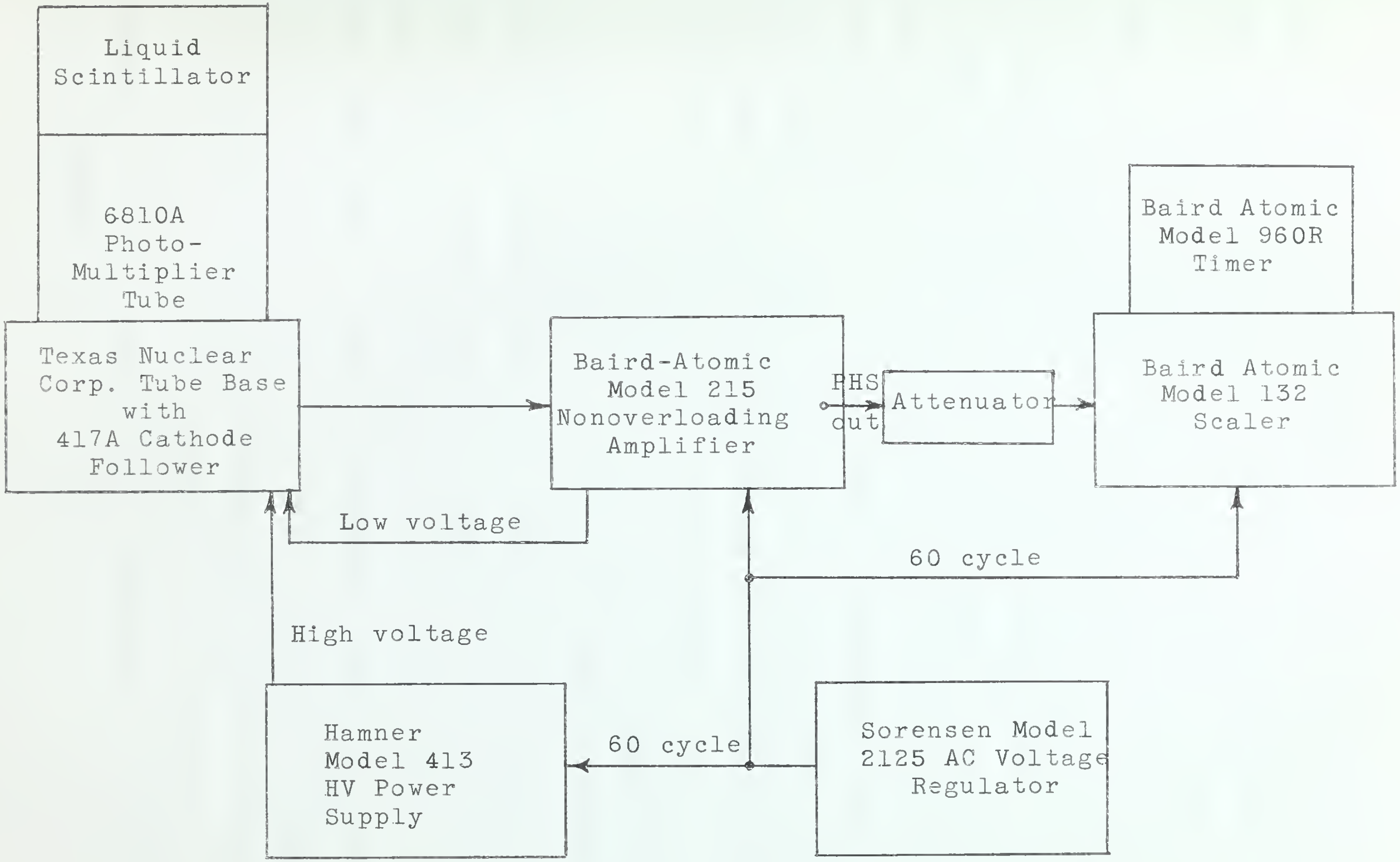
Liquid Scintillator
6810A Photo-Multiplier Tube
Texas Nuclear Corp. Tube Base with 417A Cathode Follower
Baird-Atomic Model 215 Nonoverloading Amplifier
PHS out
Attenuator
Baird Atomic Model 960R Timer
Baird Atomic Model 132 Scaler
Low voltage
60 cycle
High voltage
Hamner Model 413 HV Power Supply
60 cycle
Sorensen Model 2125 AC Voltage Regulator

Figure III-6. Block Diagram of Beta Detection and Counting Apparatus.

The factor $F_eF_{sa\&sc}(d)$ was determined experimentally by coincidence counting techniques. The various foils were irradiated long enough to reach saturation for the 2.32 hour half-life activity of Dy^{165}. Fifteen minutes were allowed to elapse between the time of removal of a foil from the irradiating flux and the time of counting. A foil was placed in the beta counting apparatus and then a gamma ray counting apparatus utilizing a NaI crystal gamma detector was positioned adjacent to the aluminum sleeve which covered the plastic scintillator for the beta counter. Gamma rays emitted coincidentally with the beta decay of Dy^{165} passed through the aluminum sleeve and some were detected by the NaI crystal.

The coincidence count, $C_{\beta-\gamma}$, was measured first. The gamma ray count, C_γ, and the beta particle counts, C_β and C_β (4π counter) were then measured for exactly the same time interval, and the observed C_γ and C_β values were projected back along the proper decay curve on semi-log graph paper in order to normalize the C_γ, C_β, and $C_{\beta-\gamma}$ counts to the same time interval. The factor $F_eF_{sa\&sc}(d)$ was then determined by dividing $C_{\beta-\gamma} \times C_\beta(4\pi$ counter) by $C_\gamma \times C_\beta$ as discussed in Chapter II. The values of $F_eF_{sa\&sc}(d)$ thus determined are tabulated with other foil data in Chapter IV.

D. Experimental Procedure

The foils were exposed, one at a time, at various locations in the radial access port of the reactor assembly at intervals of approximately 1.2 centimeters. The irradiation time for each foil was 5 minutes. After waiting 15 minutes after removal of the foil from the reactor, the beta activity from the decay of Dy^{165} was counted for a period of 10 minutes. During the 15 minute waiting period a 10 minute background count was taken and this value was assumed to be the background count during the foil counting period.

This procedure was followed for both the cadmium covered foil measurements and the bare foil measurements. The same foil was used for both measurements at a given location. During the bare foil measurement, a polyethylene spacer disc was used to replace the lower cadmium cover in order to position the foil in exactly the same location insofar as was feasible. The actual difference in location was never more than 0.33 millimeters, and since C_{cd} is only about 1 per cent of C_{th}, the error due to any difference in location was assumed to be completely negligible. The cadmium cover used was in the form of a cup with a disc which fitted completely inside the lip. The cadmium used in this cover was 0.051 centimeters thick.

The beam current (and hence the source strength) for each irradiation was determined by taking 20 beam current readings, equally spaced in time, during the 5 minute irradiation period. The average of these 20 readings was the value used for the beam current. All foil activity measurements were normalized to the same beam current of 1.5 microamperes. This amounted to normalization to an external source strength of 92.2×10^6 neutrons per second, since the source strength is directly proportional to the beam current, and since 92.2×10^6 neutrons per second is the source strength corresponding to 1.5 microamperes of deuteron beam current (see Figure III-3).

The scintillation counter was kept completely full of liquid scintillator at all times, and the liquid scintillator was changed frequently in order to prevent contamination. The foils were kept as clean as possible, and were washed in used scintillator each time prior to being inserted into the detector.

Prior to commencing measurements each day the counting system was checked for proper operation using a Na^{22} source of constant activity. This source gave a counting rate of 28090 counts per 2 minutes. The various equipment settings used were as follows:

High Voltage	1900 volts
Amplifier Discriminator . . .	080
Amplifier Gain	6400
Scalar Discriminator	0.0

Measurements were taken first with no control rod in the reactor and then with the cadmium control rod in the reactor, and lastly with the boron control rod in the reactor. The control rods were placed along the longitudinal axis and covered the entire length of the axial access port of the reactor. The effect of the boron rod was small and was not reported in this thesis.

CHAPTER IV

DATA AND GRAPHS

FOIL DATA

Foil Number	Diameter (cm)	Thickness (cm)	Weight (mg)	Thickness (mg/cm^2)	μd	$\alpha(d)$	Core $F_{sp}(d)$	Reflector $F_{sp}(d)$	$F_e F_{sa+sc}(d)$
1	1.003	0.0168	90.15	114.1	0.4019	0.4870	1.1062	1.1047	0.09892
2	1.003	0.0165	91.75	116.1	0.4089	0.4923	1.1074	1.1059	0.09807
3	1.000	0.0157	92.35	117.6	0.4142	0.4962	1.1079	1.1064	0.09764
4	1.004	0.0150	95.80	121.0	0.4262	0.5054	1.1103	1.1088	0.09498
5	1.002	0.0152	95.95	121.7	0.4287	0.5072	1.1105	1.1090	0.09415
6	1.002	0.0147	96.50	122.4	0.4311	0.5090	1.1109	1.1094	0.09378
7	1.000	0.0157	96.85	123.3	0.4343	0.5113	1.1112	1.1096	0.09482
8	1.000	0.0152	97.25	123.8	0.4361	0.5126	1.1115	1.1099	0.09496
9	1.002	0.0152	97.50	123.7	0.4357	0.5124	1.1116	1.1101	0.09554
10	1.002	0.0157	97.55	123.7	0.4357	0.5124	1.1116	1.1101	0.09613
11	1.002	0.0155	98.75	125.4	0.4417	0.5168	1.1126	1.1110	0.09337
12	1.002	0.0160	99.30	125.9	0.4435	0.5180	1.1129	1.1113	0.09448
13	1.000	0.0155	99.30	126.4	0.4452	0.5192	1.1129	1.1113	0.09483
14	1.000	0.0155	99.45	126.6	0.4459	0.5197	1.1130	1.1114	0.09298

See Chapter II for discussion of equations for $\alpha(d)$ and $F_{sp}(d)$ and for discussion of determination of $F_e F_{sa+sc}(d)$.

RADIAL DATA FOR REACTOR WITHOUT CONTROL ROD

Foil Number	Distance From Center (cm)	C_{total}*	C_{cd}*	C_{th}	$\frac{K\ F_{sp}}{F_e F_{sa+sc} m}$ ($\times 10^{-6}$)	n* $\left(\frac{\text{neutrons}}{\text{cm}^3}\right)$	n** $\left(\frac{\text{neutrons}}{\text{cm}^3}\right)$
1	2.12	490794	5780	485014	14.517	7.0410	76.366
2	3.22	465065	5522	459543	14.404	6.6191	71.790
3	4.39	419484	4836	414648	14.379	5.9622	64.665
4	5.56	386772	4206	382566	14.281	5.4634	59.255
5	6.73	341479	3712	337767	14.387	4.8595	52.706
6	7.90	297990	2773	295217	14.366	4.2411	45.998
7	9.07	261617	2436	259181	14.162	3.6705	39.810
8	10.26	209643	1901	207742	14.085	2.9260	31.735
9	11.45	180160	1645	178515	13.966	2.4931	27.040
10	12.62	177475	1402	176073	13.855	2.4395	26.458
11	13.83	158030	989	157041	14.102	2.2146	24.019
12	15.03	138148	698	137450	13.863	1.9055	20.667
13	16.23	110555	499	110056	13.811	1.5200	16.485
14	17.44	81906	360	81546	14.068	1.1472	12.442
1	19.85	47885	151	47734	14.498	0.6920	7.506
2	22.26	25289	99	25190	14.384	0.3623	3.930
3	24.67	11854	72	11782	14.360	0.1692	1.835
4	27.10	1807	86	1721	14.262	0.0245	0.266

*Normalized to source strength of 0.922×10^8 neutrons per second and corrected for background activity.

**Normalized to source strength of 1×10^9 neutrons per second.

RADIAL DATA FOR REACTOR WITH CADMIUM CONTROL ROD ALONG LONGITUDINAL AXIS

Foil Number	Distance From Center (cm)	C_{total}*	C_{cd}*	C_{th}	$\frac{K\,F_{sp}}{F_e F_{sa+sc}{}^m}$ ($\times 10^{-6}$)	n* $\left(\frac{\text{neutrons}}{\text{cm}^3}\right)$	n** $\left(\frac{\text{neutrons}}{\text{cm}^3}\right)$
1	2.12	224946	4500	220446	14.517	3.2002	34.709
2	3.22	313430	4678	308752	14.404	4.4473	48.235
3	4.39	348009	4005	344004	14.379	4.9464	53.648
4	5.56	350987	3619	347368	14.281	4.9608	53.804
5	6.73	325154	3114	322040	14.387	4.6332	50.251
6	7.90	282806	2664	280142	14.366	4.0245	43.649
7	9.07	244425	2023	242402	14.162	3.4329	37.233
8	10.26	192897	1425	191472	14.085	2.6969	29.250
9	11.45	160157	1201	158956	13.966	2.2200	24.078
10	12.62	159154	1199	157955	13.855	2.1885	23.736
11	13.83	139600	915	138658	14.102	1.9554	21.208
12	15.03	129714	614	129100	13.863	1.7911	19.426
13	16.23	104507	403	104104	13.811	1.4378	15.594
14	17.44	78057	267	77790	14.068	1.0943	11.869
5	19.85	40301	162	40139	14.368	0.5767	6.255
6	22.26	20985	92	20893	13.942	0.2913	3.159
7	24.67	9837	76	9761	14.141	0.1380	1.497
8	27.10	1762	31	1731	14.066	0.0244	0.264

*Normalized to source strength of 0.922 × 10^8 neutrons per second and corrected for background activity.

**Normalized to source strength of 1 × 10^9 neutrons per second.

CORE-REFLECTOR INTERFACE DATA

Foil Number	Distance From Midplane (cm)	C_{th}*	$\frac{K\,F_{sp}}{F_e F_{sa+sc}^{m}}$ ($\times 10^{-6}$)	n $\left(\frac{\text{neutrons}}{\text{cm}^3}\right)$	n** $\left(\frac{\text{neutrons}}{\text{cm}^3}\right)$
6	3.16	95441	13.942	1.3306	14.431
7	6.35	81115	14.141	1.1470	12.440
8	9.52	62244	14.066	0.8755	9.496
9	12.70	49795	13.947	0.6945	7.533
10	15.88	35864	13.855	0.4969	5.389
	Distance From Longitudinal Center Line (cm)				
11	11.43	31418	14.102	0.4431	4.806
12	8.89	36852	13.863	0.5109	5.541
13	6.35	47622	13.811	0.6577	7.133
14	3.81	61058	14.068	0.8590	9.317

*Normalized to source strength of 0.922 × 10^8 neutrons per second and corrected for background activity.

**Normalized to source strength of 1 × 10^9 neutrons per second.

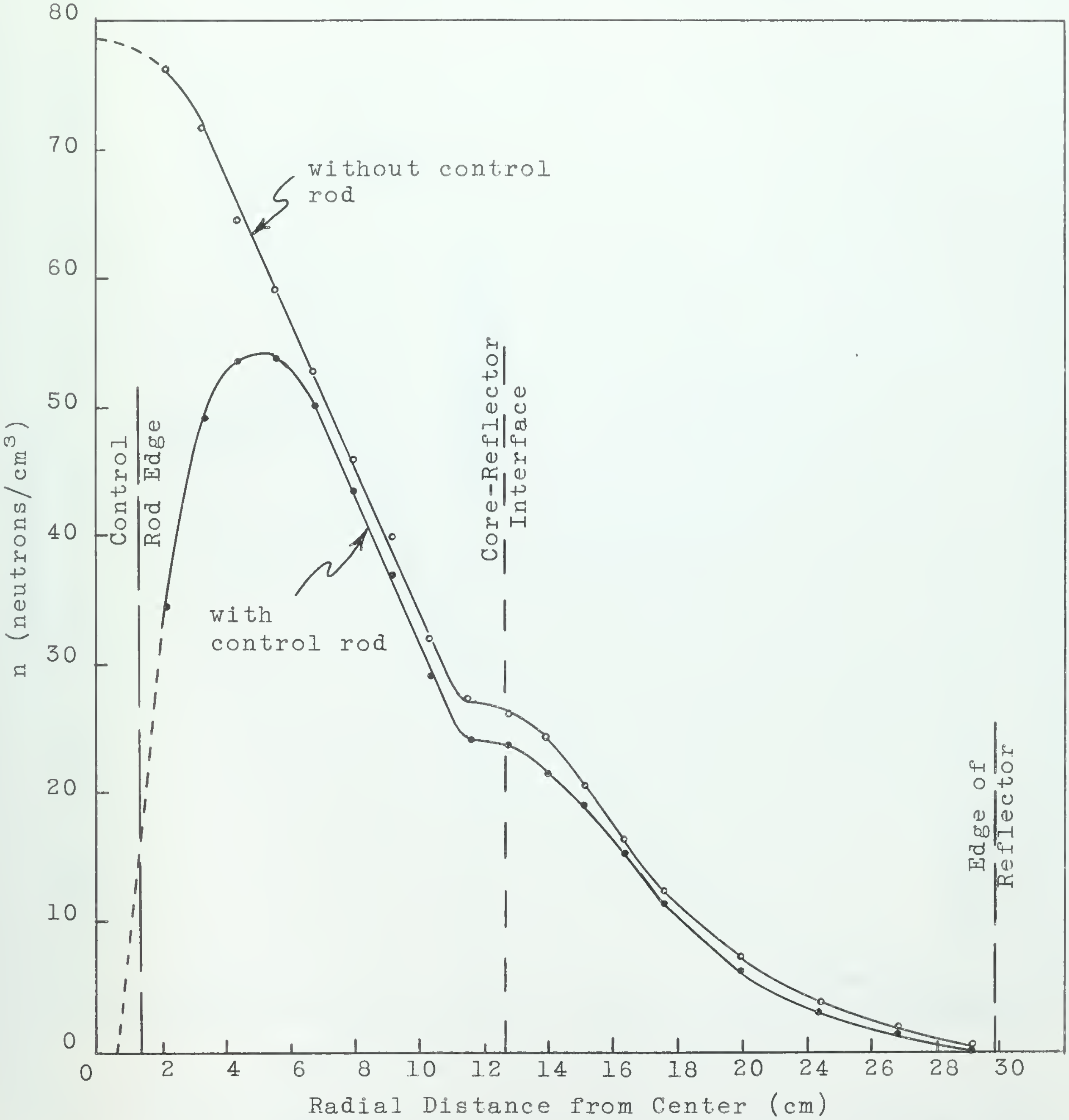

Figure IV-1. Radial Neutron Density Distribution (Experimental).

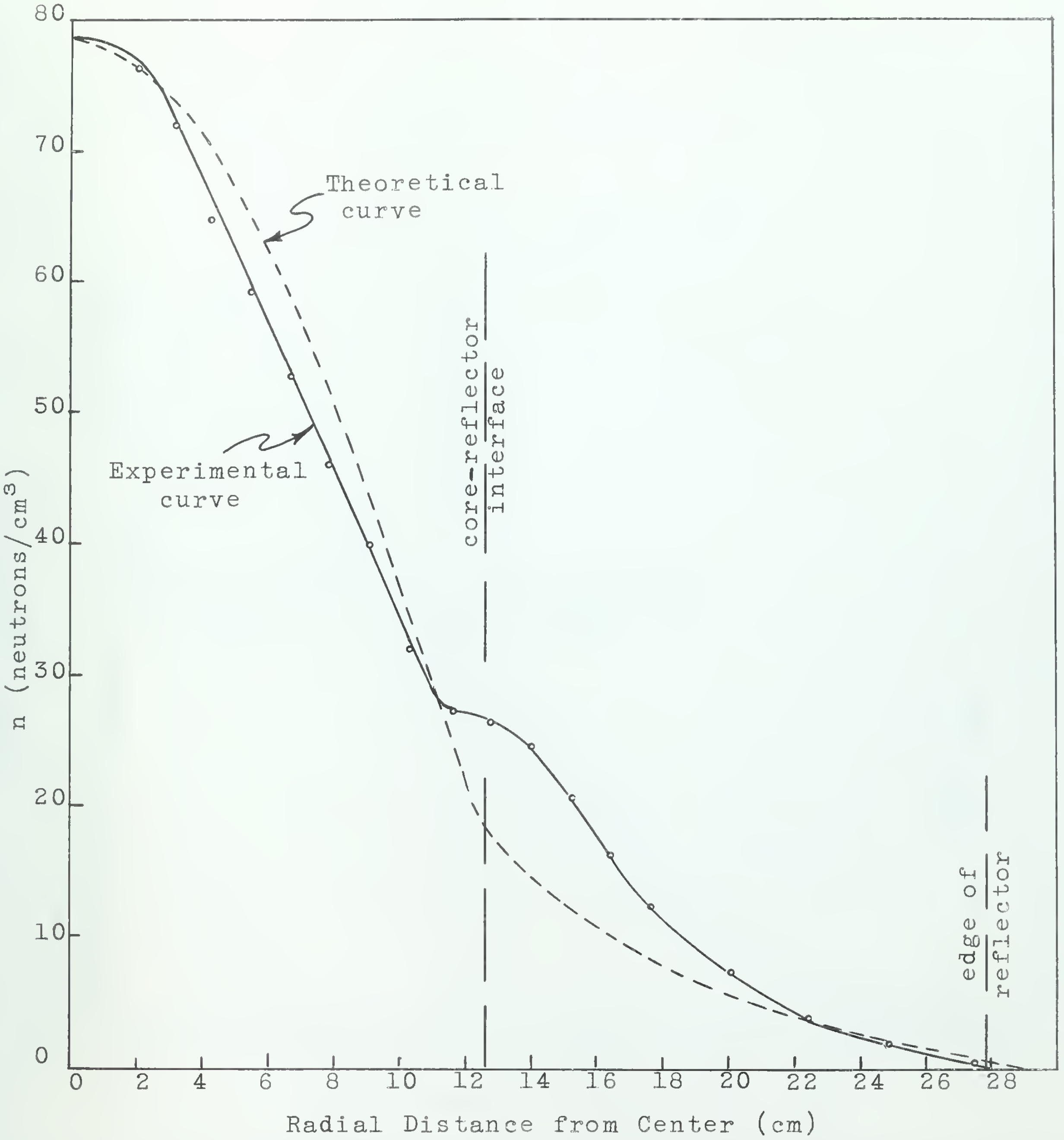

Figure IV-2. Comparison of Theoretical and Experimental Radial Neutron Density Distribution Curves without Control Rod.

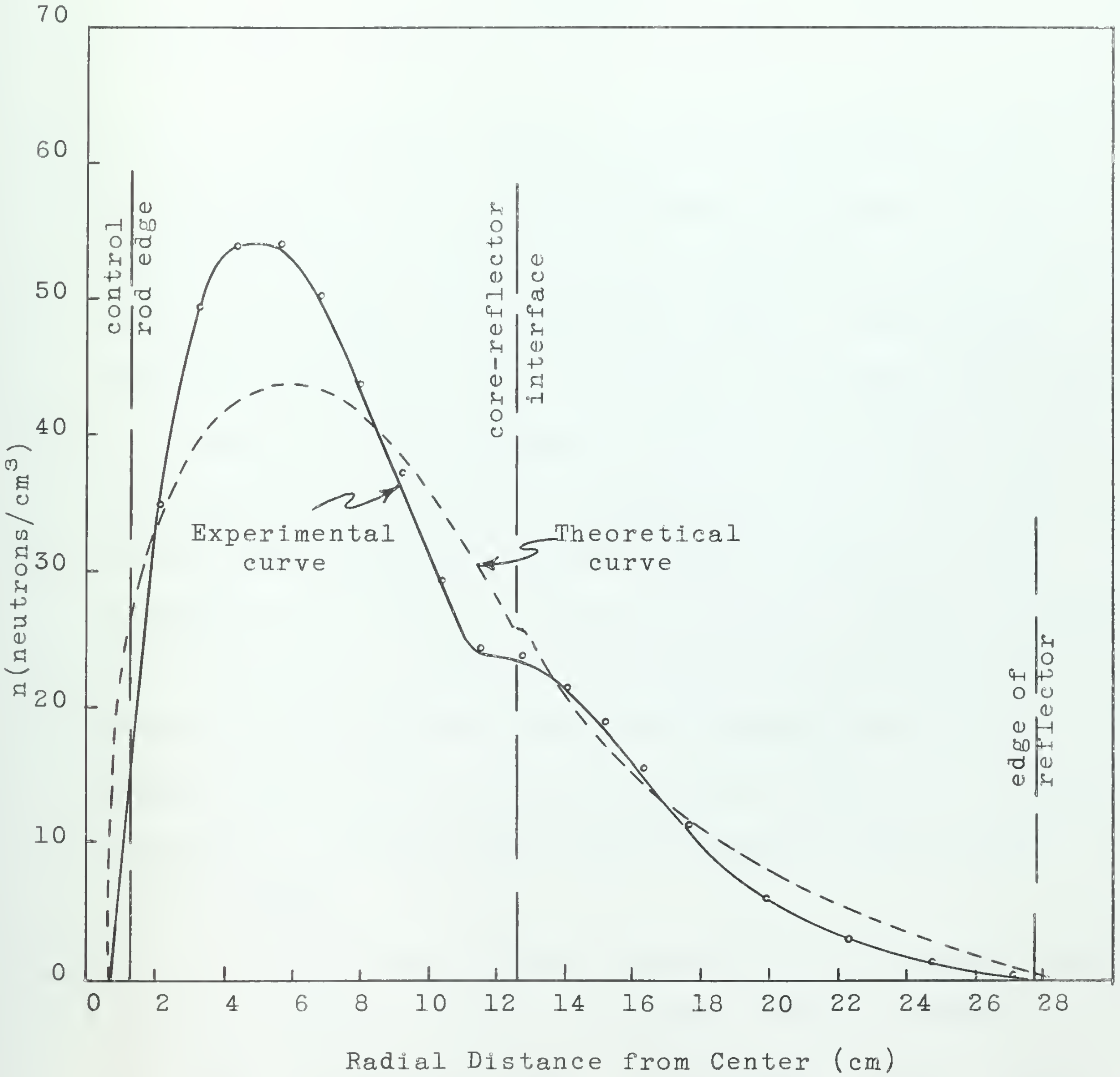

Figure IV-3. Comparison of Theoretical and Experimental Radial Neutron Density Distribution Curves with Control Rod.

CHAPTER V

RESULTS

The radial neutron density distribution curves as determined by experimental methods are shown in Figure IV-1 for the reactor with and without the control rod in position along the longitudinal axis of the assembly. The neutron density values shown here have been normalized to a constant source strength of 10^9 neutrons per second from the Be(d,n) reaction. Comparison of the two curves shows a large depression of the neutron density in the vicinity of the control rod and a general decrease throughout the reactor. This is to be expected since the large number of neutrons absorbed by the cadmium rod are no longer available to diffuse through the reactor or to participate in fission events which release other neutrons to the system.

The single velocity group diffusion theory technique was used to predict the neutron density distribution for each case mathematically. The results of this treatment are shown graphically in Figure IV-2 for the reactor with no control rod and in Figure IV-3 for the reactor with

the control rod. The agreement between the theoretical and experimental distributions could be termed no better than fair in either case.

The large "hump" observed experimentally at the boundary between the core and the reflector is not adequately represented by the theoretical distributions, although a slight change in slope is indicated at that position. It is interesting to note, however, that the areas under the theoretical curves are essentially the same as the areas under the corresponding experimental curves. This implies that the theory does provide for the proper total number of neutrons although the distribution is somewhat distorted.

It is believed that the agreement between the distributions predicted by diffusion theory and those observed experimentally would have been better if a more accurate value had been available for the buckling of the reactor used in this experiment. Calculations show that, if the value $B_c^2 = 0.02\text{cm}^{-2}$ were used in this case, the neutron density predicted theoretically for the core-reflector interface would have been almost exactly the same as that experimentally observed.

Analysis of the data obtained for various positions at the core-reflector interface indicate that surfaces

of equal neutron density would have the form of an ellipsoid of revolution with a ratio of major and minor semiaxes of approximately 1.2 to 1. This implies that, if the change in slope at the core-reflector interface were neglected, theoretical calculations for the system might be made with considerable success using spherical geometry. Calculations involving spherical coordinates are, of course, much more simple than are those involving cylindrical coordinates.

APPENDIX A

REACTOR CONSTANTS AND CALCULATIONS

Core Dimensions*

Fuel Element Number	Thickness (inches)	Diameter (inches)	Hole Diameter (inches)	Volume (cubic inches)
1	1.900	9.913	1.282	144.18
2	2.050	9.908	1.286	155.38
3	2.070	9.906	1.280	156.84
4	2.070	9.905	1.280	156.84
5	2.045	9.912	1.280	155.17
6	2.057	9.934	1.282	156.76
7	1.035	9.931	1.280	78.84
8		NOT USED		
9	0.507	9.920	1.283	38.52
10		NOT USED		
			Total Volume	= 1,042.54

Expressed in Terms of Cubic Centimeters, Centimeters, and Grams.

Total Volume = 17,090.36 cm^3
Average Diameter = 9.914 in. = 25.182 cm
Total Thickness = 13.734 in. = 34.884 cm
Total Weight of Core = 18,603.2 grams
Core Density = 1.08852 $grams/cm^3$
Total Weight of UO_2 in Core = 2,668.49 grams
Total Weight of U^{235} in Core = 465.04 grams
Total Weight of U in Core = 2,351.54 grams

---

*Data furnished by manufacturer, Lockheed Aircraft Corp., Marietta, Ga.

Core Constants* (density = 1.08852 gm/cm^3)

Element	N (atoms/cm^3)	σ_s (barns)	σ_a (barns)	σ_f (barns)	Σ_s (cm^{-1})	Σ_a (cm^{-1})	Σ_{tot} (cm^{-1})	$(\cos\theta)_{avg}$ $\left(= \frac{2}{3A}\right)$	Σ_{tr} (cm^{-1})	Σ_f (cm^{-1})	ξ
H'	8.025 x 10^{22}	38.0	0.332	0	3.0495	0.0266	3.0761	0.6667	1.0430	0	1.0000
C^{12}	4.0125 x 10^{22}	4.8	0.0034	0	0.1926	0.0001	0.1927	0.0556	0.1820	0	0.1572
O^{16}	6.984 x 10^{20}	4.2	0.0002	0	0.0029	0.0000	0.0029	0.0417	0.0028	0	0.1205
U^{235}	0.698 x 10^{20}	10.0	683.0	582.0	0.0007	0.0477	0.0484	0.0028	0.0484	0.0406	0.0121
U^{238}	2.794 x 10^{20}	8.2	2.71	0.0005	0.0022	0.0008	0.0030	0.0028	0.0030	0.0000	0.0112
TOTALS					3.2479	0.0752	3.3231		1.2792	0.0406	

* All cross sections are for thermal neutrons and are taken from Hughes, D. J., and Schwartz, R. L., Neutron Cross Sections BNL 325, U.S. Govt. Printing Office, Washington 25, D. C., July, 1958.

Reflector Constants* (density = 0.95997 gm/cm^3)

Element	N ($atoms/cm^3$)	σ_s (barns)	σ_a (barns)	Σ_s (cm^{-1})	Σ_a (cm^{-1})	Σ_{tot} (cm^{-1})	$(\cos\theta)_{avg}$ (= 2/3A)	Σ_s 2/3A (cm^{-1})	$\Sigma_{tr}(cm^{-1})$ $(=\Sigma_t-\Sigma_s \frac{2}{3A})$
H'	8.2626×10^{22}	38.0	0.332	3.1398	0.0274	3.1672	0.6667	2.0933	1.0739
C^{12}	4.1313×10^{22}	4.8	0.0034	0.1983	0.0001	0.1984	0.0556	0.0110	0.1874
TOTALS				3.3381	0.0275	3.3656		2.1043	1.2613

* All cross sections are for thermal neutrons and are taken from Hughes, D. J., and Schwartz, R. L., Neutron Cross Sections BNL 325, U.S. Govt. Printing Office, Washington, 25, D. C., July, 1958.

REACTOR CALCULATIONS[14]

The transport mean free path, λ_{tr}, for a medium is given by the equation

$$\lambda_{tr} = \frac{1}{\Sigma_{tr}} = \frac{1}{\Sigma_{total} - \Sigma_s \ (2/3A)}$$

where

$$\Sigma_{tr} = \Sigma_{total} - \Sigma_s \frac{2}{3A} = \sum \left[\Sigma_{total}^{(i)} - \Sigma_s^{(i)} \frac{2}{3A_i}\right]$$

for the i elements of which the medium is composed. Thus, for the reactor core,

$$\lambda_{tr}^{(c)} = \frac{1}{\Sigma_{tr}^{(c)}} = \frac{1}{1.2792 \text{ cm}^{-1}} = 0.78174 \text{ cm} .$$

By the same method λ_{tr} for the reflector is

$$\lambda_{tr}^{(R)} = \frac{1}{\Sigma_{tr}^{(R)}} = \frac{1}{1.2613 \text{ cm}^{-1}} = 0.79283 \text{ cm}.$$

---

[14] Meghreglian and Holmes, Reactor Analysis (New York: McGraw-Hill Book Co., 1960), Chap. 5.

The diffusion coefficient, D, for a medium is given by the equation

$$D = \frac{\lambda_{tr}}{3}$$

where λ_{tr} is the transport mean free path. For the core D_c is

$$D_c = \frac{\lambda_{tr}^{(c)}}{3} = \frac{0.78174 \text{ cm}}{3} = 0.26058 \text{ cm}$$

and for the reflector, D_R is

$$D = \frac{\lambda_{tr}^{(R)}}{3} = \frac{0.79283 \text{ cm}}{3} = 0.26428 \text{ cm.}$$

The extrapolated radius ρ_o at which ϕ becomes zero is

$$\rho_o = \rho_{measured} + 2D_R = 28.32 \text{ cm.}$$

The extrapolated height z_o at which ϕ becomes zero is

$$z_o = z_{measured} + 2D_R = 33.55 \text{ cm.}$$

The values of ρ and z at the interface between the core and the reflector are

$$\rho_i = 12.59 \text{ cm}$$

and

$$z_i = 17.44 \text{ cm}.$$

The diffusion length, L, is defined by the equation $L^2 \equiv D/\Sigma_a$. Thus, for the core,

$$L_c^2 = \frac{D}{\Sigma_a^{(c)}} = \frac{0.26058 \text{ cm}}{0.0752 \text{ cm}^{-1}} = 3.465 \text{ cm}^2 \quad ,$$

and for the reflector

$$L_R^2 = \frac{D}{\Sigma_a^{(R)}} = \frac{0.26428 \text{ cm}}{0.0275 \text{ cm}^{-1}} = 9.610 \text{ cm}^2 \; .$$

The constant κ_R^2 is defined by the equation $\kappa_R^2 \equiv 1/L_R^2$. Thus, for the reflector

$$\kappa_R^2 = \frac{1}{L_R^2} = \frac{\Sigma_a^{(R)}}{D_R} = 0.1041 \text{ cm}^{-2} \; .$$

In Chapter I it was determined that $\kappa_z = \pi/2z_o$. Thus, for the reactor used in this experiment

$$\kappa_z = \frac{\pi}{2z_o} = 0.0468 \text{ cm}^{-1} .$$

Since κ_R^2 is defined to be $\kappa_R^2 = \kappa_\rho^2 - \kappa_z^2$, the term κ_ρ can be determined as follows:

$$\kappa_\rho = \sqrt{\kappa_R^2 + \kappa_z^2} = \sqrt{0.01084 + 0.00219} = 0.11415 \text{ cm}^{-1}.$$

In order to determine k_z, the equation

$$k_z \tan k_z z_i = \frac{\pi}{2z_o} \frac{D_R}{D_c} \tan \frac{\pi}{2z_o} z_i$$

must be solved by numerical methods. This solution yields a value of

$$k_z = 0.0471 \text{ cm}^{-1} .$$

Using the value of B_c^2 furnished by the manufacturer of the reactor, k_ρ, can now be determined by the equation

$$k_\rho = \sqrt{B_c^2 - k_z^2} .$$

Since $B^2 = 0.027172 \text{ cm}^{-2}$, this relationship gives the value of

$$k_\rho = 0.1580 \text{ cm}^{-1}.$$

Evaluation of constants involving Bessel Functions at ρ_o and b_o are as follows:

$$\frac{K_o(\kappa_\rho\rho_o)}{I_o(\kappa_\rho\rho_o)} = \frac{K_o(3.233)}{I_o(3.233)} = 0.0045$$

$$b_o = b - \epsilon = 0.95 \text{ cm} - 0.71 \text{ cm} = 0.24 \text{ cm}.$$

$$\frac{J_o(k_\rho b_o)}{Y_o(k_\rho b_o)} = \frac{J_o(0.0379)}{Y_o(0.0379)} = - 0.465.$$

For the case with no control rod, where A_c = 78.7 n/cm^3 when $\rho = z = 0$, the constant C_R is evaluated as follows:

$$C_R = A_c \frac{J_o(k_\rho\rho_i)}{\left[K_o(\kappa_\rho\rho_i) - \dfrac{K_o(\kappa_\rho\rho_o)}{I_o(\kappa_\rho\rho_o)} I_o(\kappa_\rho\rho_i)\right]}$$

$$= 78.7 \frac{J_o(1.989)}{[K_o(1.4371) - 0.0045\ I_o(1.4371)]} \quad \text{n/cm}^3$$

giving C_R = 80.56 n/cm^3.

When the control rod is in position, A_c is taken to be the maximum experimental value in order to correlate experiment and theory. This gives the value A_c = 54.3 n/cm^3.

Using this value, C_R can be evaluated by the relationship

$$C_R = A_c \frac{\left[J_o(k_p\rho_i) - \frac{J_o(k_\rho b_o)}{Y_o(k_\rho b_o)} Y_o(k_\rho\rho_i)\right]}{\left[K_o(\kappa_\rho\rho_i) - \frac{K_o(\kappa_\rho\rho_o)}{I_o(\kappa_\rho\rho_o)} I_o(\kappa_\rho\rho_i)\right]}$$

$$= 54.3 \frac{[J_o(1.989) + 0.465\ Y_o(1.989)]}{[K_o(1.437) - 0.0045\ I_o(1.437)]} \quad n/cm^3$$

giving $C_R = 112.73\ n/cm^3$.

In summary, the equations for $n(\rho,z)$ with all the constants evaluated are as follows:

(a) Without control rod:

$$n_c(\rho,z) = 78.7\ J_o(0.158\rho) \cos 0.0471z$$

$$n_R(\rho,z) = 80.56[K_o(0.1142\rho) - 0.0045I_o(0.1142\rho)] \times \cos 0.0468z$$

(b) With control rod:

$$n_c(\rho,z) = 54.3[J_o(0.158\rho) + 0.465Y_o(0.158\rho)]\cos 0.471z$$

$$n_R(\rho,z) = 112.73[K_o(0.1142\rho) - 0.0045I_o(0.1142\rho)] \times \cos 0.0468z$$

These equations were used to determine the theoretical neutron density distribution curves shown in Figures IV-2 and IV-3.

APPENDIX B

PROBABLE ERROR

The probable error of a function F(x,y,z) is given by[15]

$$P_F = \sqrt{\left(P_x \frac{\partial F}{\partial x}\right)^2 + \left(P_y \frac{\partial F}{\partial y}\right)^2 + \left(P_z \frac{\partial F}{\partial z}\right)^2}$$

where P_x, P_y, and P_z are the probable errors in x, y, and z, respectively. The probable errors P_x, P_y, and P_z are defined by the general equation

$$P_q = 0.6745\sigma$$

where σ is the standard deviation of the value observed.

The function, n(ρ,z), with which this experiment is concerned, is related to the measured quantities by the equation

$$n(\rho,z) = \frac{K\ C_{th}\ F_{sp}\ (d)}{m\ F_e\ F_{sa\&sc}(d)}$$

where K is a constant having the value

---

[15] H. Margenau and G. M. Murphy, The Mathematics of Physics and Chemistry (2d ed.; Princeton, N.J.: D. Van Nostrand Co., 1956), Sections 13.32-36.

$$K = \frac{1 \times 10^9}{2.2 \times 10^5 \times 38.412 \times 1.011 \times 92.2 \times 10^6} = 0.1269 \times 10^{-5}$$

when source strength of 1 × 10^9 neutrons per second is used.

The probable error for $n(\rho,z)$ can thus be written

$$\text{Eq. (1):}\quad P_n = K\left\{\left(P_{C_{th}} \frac{F_{sp}}{m\ F_e\ F_{sa\&sc}}\right)^2 + \left(P_{F_{sp}} \frac{C_{th}}{m\ F_e\ F_{sa\&sc}}\right)^2\right.$$

$$\left. + \left(P_m \frac{C_{th}F_{sp}}{m^2\ F_e\ F_{sa\&sc}}\right)^2 + \left(P_{F_eF_{sa\&sc}} \frac{C_{th}F_{sp}}{m\ F_e^2\ F_{sa\&sc}^2}\right)^2\right\}^{\frac{1}{2}}$$

assuming K has no error.

The data obtained experimentally for the point $\rho = 12.62$ cm, $z = 0$ will be used to determine the probable error for this experiment.

The value C_{th} is obtained by the relation

$$C_{th} = C_{total} - C_{cd}$$

where C_{total} and C_{cd} are measured quantities. The probable error $P_{c_{th}}$ is

$$P_{C_{th}} = \sqrt{P_{C_{total}}^2 + P_{C_{cd}}^2}$$

where

$$P^2_{C_{total}} = [0.6745\sqrt{177475}]^2 = 81,134$$

and

$$P^2_{C_{cd}} = [0.6745\sqrt{1402}]^2 = 640.$$

Thus

$$P_{C_{th}} = \sqrt{81134 + 640} = 286.$$

The probable error in $F_{sp}(d)$ is called $P_{F_{sp}}$ and use of the average error of 1.5 per cent tabulated by Tittle[16] for the function $F_{sp}(d)$ gives $P_{F_{sp}} = 0.01665$.

The probable error in the foil weight, P_m, is 0.0001 grams.

The probable error $P_{F_e F_{sa\&sc}}$ for the self absorption and self scattering correction factor is determined by the relation

---

[16] C. W. Tittle, Physical Review, 80, p. 756, 1950.

$$P_{F_eF_{sa\&sc}} = \ell \left\{\left[\left(P_{C_{\beta-\gamma}} \frac{C_{\beta}(4\pi)}{C_{\beta}C_{\gamma}}\right)^2 + \left(P_{C_{\beta}(4\pi)} \frac{C_{\beta-\gamma}}{C_{\beta}C_{\gamma}}\right)^2 + \left(P_{C_{\beta}} \frac{C_{\beta-\gamma}C_{\beta}(4\pi)}{C_{\beta}^2C_{\gamma}}\right)^2 + \left(P_{C_{\gamma}} \frac{C_{\beta-\gamma}C_{\beta}(4\pi)}{C_{\beta}C_{\gamma}^2}\right)^2\right]\right\}^{\frac{1}{2}}$$

since $F_eF_{sa\&sc} = \ell \dfrac{C_{\beta-\gamma}C_{\beta}(4\pi)}{C_{\beta}C_{\gamma}}$ where ℓ is a constant having the value $\ell = 0.8962$. Using the values

$$P_{C_i} = 0.6745\sqrt{C_i}$$

in the above relation gives

$$P_{F_eF_{se\&sc}} = 0.000866.$$

Thus, the total probable error is determined to be, using equation (1),

$$P_n(\text{experimental}) = 0.466\ n/cm^3,$$

most of which can be attributed to the low $C_{\beta-\gamma}$ count rates experienced when experimental determination of $F_eF_{sa\&sc}(d)$ was accomplished, and to the probable error in F_{sp}.

This value represents a total probable error of

$$P_n(\text{experimental}) = 1.77 \text{ per cent}$$

for the neutron density values determined in this experiment.

The probable errors in the constant terms used in the development of the expression for neutron density are those given by the authors making the determinations and are:

$$P_{\sigma_{n\gamma}^{4-5}} = 100 \text{ barns for } \sigma_{n\gamma}^{4-5} = 800 \text{ barns}$$

$$P_{\sigma_{n\gamma}^{4-5m}} = 200 \text{ barns for } \sigma_{n\gamma}^{4-5m} = 2000 \text{ barns.}$$

BIBLIOGRAPHY

BIBLIOGRAPHY

Bonilla, C. F. Nuclear Engineering, McGraw-Hill Book Company, New York, 1957.

Doss, T. T. Unpublished Thesis, The University of Texas, Austin, Texas, June, 1961.

Eichenbaum, F. D. Lockheed Nuclear Products Reports NR 57 and 58, Nuclear Products Division of Lockheed Aircraft Corporation, Marietta, Georgia, March, 1959.

Glasstone, S. Sourcebook on Atomic Energy, Second Edition, D. Van Nostrand Company, Princeton, N.J., 1958.

Glasstone, S. Principles of Nuclear Reactor Engineering, D. Van Nostrand Company, Princeton, N.J., 1955.

Greenfield, M. A., et al. Nucleonics, 15, No. 3, March, 1957.

Hughes, D. J., and Schwartz, R. B. Neutron Cross Sections, BNL 325, U.S. Government Printing Office, Washington 25, D.C., July, 1958.

Hughes, D. J., et al. Neutron Cross Sections, Supplement No. 1 to BNL 325, U.S. Government Printing Office, Washington 25, D.C., January, 1960.

Jahnke, E., and Emde, F. Tables of Functions, Dover Publishing Company, New York, 1943.

Margenau, H., and Murphy, G. M. The Mathematics of Physics and Chemistry, 2nd Edition, D. Van Nostrand Company, Princeton, N.J., 1956.

Meghreblian, R. V., and Holmes, D. K. Reactor Analysis, McGraw-Hill Book Company, New York, 1960.

Shpetnyi, A. I. Soviet Physics JETP, 5, October, 1957.

Tittle, C. W. Nucleonics, 8, No. 6, June, 1951.

Tittle, C. W. Nucleonics, 9, No. 1, July, 1951.

Tittle, C. W. Physical Review, 80, 1950.

Tornau, R. Zeitschrift fur Physik, 159, 1960.

VITA

Richard W. Reed was born in Winston-Salem, North Carolina, on February 26, 1930, the son of Watemon T. Reed and Bess K. Reed. He attended public schools in Winston-Salem, graduating from high school in 1948. He entered Alabama Polytechnic Institute (now Auburn University) in September, 1948, and received the degree of Bachelor of Science in Electrical Engineering from that institution in August, 1952, at which time he also received a commission in the U. S. Navy. After serving in the Navy for three years, he entered North Carolina State College in September, 1955, for work in Industrial Engineering. Prior to receipt of a degree from N. C. State College, he re-entered the Navy and is currently on active duty with the rank of Lieutenant Commander. In September, 1959, Lcdr. Reed was sent by the Navy to Rice Institute (now Rice University) for graduate study in Nuclear Physics, and after one year at Rice, he was transferred to the University of Texas.

Permanent Address: 1124 Second Street
Gulfport, Mississippi

Typing by

Martha Ann Zivley Typing Service
2013 Guadalupe Street
Austin, Texas

thesR2698
Effect of a cadmium control rod on the n
3 2768 002 05025 4
DUDLEY KNOX LIBRARY